1 **Land-atmosphere interactions in the tropics – a review**

3 Pierre Gentine

4 *Department of Earth and Environmental Engineering,*

5 *Earth Institute*

6 *Columbia University, New York, NY, USA*

8 Adam Massmann

9 *Department of Earth and Environmental Engineering,*

10 *Earth Institute*

11 *Columbia University, New York, NY, USA*

13 Benjamin R. Lintner

14 *Department of Environmental Sciences*

15 *Rutgers, The State University of New Jersey, New Brunswick, NJ, USA*

17 Sayed Hamed Alemohammad

18 *Department of Earth and Environmental Engineering,*

19 *Earth Institute,*

20 *Columbia University, New York, NY, USA*

22 Rong Fu

23 *Department of Atmospheric and Ocean Sciences*

24 *University of California, Los Angeles, Los Angeles, CA, USA*

26 Julia K. Green

27 *Department of Earth and Environmental Engineering,*

28 *Earth Institute,*

29   *Columbia University, New York, NY, USA*

31 Daniel Kennedy

32   *Department of Earth and Environmental Engineering,*

33   *Earth Institute,*

34   *Columbia University, New York, NY, USA*

36   Jordi Vilà-Guerau de Arellano

37   *Meteorology and Air Quality Group*

38   *Wageningen University, Wageningen, the Netherlands*

40   Revised for *HESS*, 31 July 2019

44   ______________________

46   *Corresponding author address:* Pierre Gentine, Department of Earth and Environmental

47   Engineering, Columbia University, NY 10027, USA.

48   E-mail: pg23288@columbia.edu

49   Phone number: +1-212-854-7287

ABSTRACT

The continental tropics play a leading role in the terrestrial energy, water, and carbon cycles. Land-atmosphere interactions are integral in the regulation of these fluxes across multiple spatial and temporal scales over tropical continents. We review here some of the important characteristics of tropical continental climates and how land-atmosphere interactions regulate them. Along with a wide range of climates, the tropics manifest a diverse array of land-atmosphere interactions. Broadly speaking, in tropical rainforest climates, light and energy are typically more limiting than precipitation and water supply for photosynthesis and evapotranspiration, whereas in savanna and semi-arid climates, water is the critical regulator of surface fluxes and land-atmosphere interactions. We discuss the impact of the land surface, how it affects shallow and deep clouds and how these clouds in turn can feed back to the surface by modulating surface radiation and precipitation. Some results from recent research suggest that shallow clouds may be especially critical to land-atmosphere interactions. On the other hand, the impact of land surface conditions on deep convection appears to occur over larger, non-local, scales and may be a more relevant land-atmosphere feedback mechanism in transitional dry to wet regions and climate regimes.

1   Introduction

The Tropics play a substantial role in regulating the global hydrologic and carbon cycles. Tropical rainforests are one of the main terrestrial carbon sinks [*Nakicenovic*, 2000; *Friedlingstein et al.*, 2006] but their projected responses to a warming climate remain unclear because of uncertainties associated with the representation of abiotic and biotic processes in models as well as confounding factors such as deforestation and changes in land use and land cover [*Wang et al.*, 2009; *Davidson et al.*, 2012; *Fu et al.*, 2013; *Saatchi et al.*, 2013; *Hilker et al.*, 2014; *Boisier et al.*, 2015; *Doughty et al.*, 2015; *Gatti et al.*, 2015; *Knox et al.*, 2015; *Saleska et al.*, 2016]. The ecosystems of tropical monsoonal and seasonal wet-dry climates are also important contributors to the global carbon cycle, especially with respect to the interannual variability of the tropical terrestrial carbon sink [*Poulter et al.*, 2014; *Jung et al.*, 2017; *Green et al.*, 2019].

79   Some regions of the tropics have been further identified as hotspots in which land-
80   atmosphere interactions modify the climate [*Dirmeyer et al.*, 2011; *Koster et al.*, 2011;
81   *Green et al.*, 2017] either locally, i.e. at horizontal scales on the order of a few boundary
82   layer heights, regionally, at scales up to a few hundreds of kilometers, or at larger scales,
83   over several of thousands of kilometers, through coupling between the surface and the
84   overlying atmosphere [*Lintner and Neelin*, 2009]. These interactions may in turn
85   dramatically affect the future state of rainforests [*Cox et al.,* 2004].

86

87   While tropical land-atmosphere interactions are often examined through the lens of
88   coupling between land surface states (e.g., soil moisture) and rainfall, other aspects of the
89   coupling are also important. For example, even under nonprecipitating conditions,
90   surface radiation, temperature and vapor pressure deficit (VPD) may be altered [*Lawton*
91   *et al.*, 2001; *Pielke et al.*, 2016; *Green et al.*, 2017] through coupling with clouds,
92   aerosols and shallow (non-precipitating) convection [*Avissar and Nobre*, 2002; *Medvigy*
93   *et al.*, 2011; *Seneviratne*, 2013; *Cook et al.*, 2014; *Guillod et al.*, 2015; *Krakauer et al.*,
94   2016; *Martin et al.*, 2016; *Green et al.*, 2017; *Khanna et al.*, 2017; *Martin et al.*, 2017;
95   *Thiery et al.*, 2017; *Vogel et al.*, 2017]. In addition, tropical forests can exhibit important
96   variations in canopy photosynthetic capacity with new leaves [*Lopez et al.*, 2016; *Saleska*
97   *et al.,* 2003, 2016]. These variations can further feed back onto the atmosphere on
98   seasonal time scales [*Green et al.*, 2017]. It is clear that the tropical energy, water, and
99   carbon cycles cannot be understood in isolation; rather, the interactions among these
100   cycles are essential. For example, knowledge of such interactions must be taken into
101   account to ascertain whether the terrestrial tropics will act as a future carbon sink or
102   source [*Zhang et al.*, 2015; *Swann et al.*, 2015].

103

104   The two-way interactions that occur between the land surface and overlying atmosphere
105   represent one of the more uncertain aspects of the terrestrial climate system, particularly
106   in the Tropics [*Betts and Silva Dias*, 2010]. While the land surface is widely recognized
107   as integral to the occurrence of important tropical climate phenomena such as monsoons
108   [*Zeng and Neelin*, 1999; *Zeng et al.*, 1999], isolating and quantifying its precise role
109   remains elusive. Indeed, such efforts have frequently been hampered by the paucity of

110 observational data, not to mention the complex and multiple pathways through which
111 land-atmosphere interactions can take place.

112

113 Several notable field campaigns have been conducted in the tropics with the purpose of
114 advancing knowledge of land-atmosphere interactions. One of the most well-known
115 campaigns was the Large-Scale Biosphere-Atmosphere Experiment in Amazonia (LBA)
116 [*Avissar et al.*, 2002; *Keller et al.*, 2004], which aimed at refining our understanding of
117 climatological, hydrological, biogeochemical and ecological processes of the Amazon
118 and their linkages, in addition to the anthropogenic impacts (e.g., land-use land cover
119 changes and deforestation) on these. Among many other topics, LBA generated
120 fundamental insights on the structure of the tropical atmosphere, processes generating
121 precipitation, and the seasonal variability of surface turbulent fluxes in tropical
122 rainforests [*Avissar and Nobre*, 2002; *Betts et al.*, 2002; *Laurent et al.*, 2002; *Machado*
123 *and Laurent*, 2002; *Acevedo et al.*, 2004; *Khairoutdinov and Randall*, 2006; *Fitzjarrald*,
124 2007; *Juárez et al.*, 2007; *Restrepo-Coupe et al.*, 2013]. One thrust of LBA research
125 sought to isolate the effect of deforestation on precipitation, both in a local context as
126 well as remotely via teleconnections [*Avissar et al.,* 2002; *Werth and Avissar*, 2002].
127 Such research has pointed to deforestation decreasing precipitation, albeit with uncertain
128 magnitude and dependence on the spatial scales involved. Even now, two decades after
129 the inception of LBA, the relationship between tropical deforestation and precipitation
130 remains uncertain, despite progress with respect to key processes such as vegetation
131 access to deep water in the dry season [*Oliveira et al.* 2005], and modulation of energy
132 availability for photosynthesis via cloud cover [*Betts and Dias*, 2010].

133

134 Another field campaign, the African Monsoon Multidisciplinary Analysis (AMMA)
135 campaign, focused on the West African monsoon system, especially the Sahel transition
136 zone [*Redelsperger et al.*, 2006; *Boone et al.*, 2009b]. Building on previous field work in
137 the region [*e.g. HAPEX-Sahel*, *Gourtorbe et al. 1993*], AMMA generated fundamental
138 understanding of mesoscale convective systems and surface processes [*Lebel et al.*, 2009;
139 *Taylor et al.*, 2009; *Boone et al.*, 2009a; *Lohou et al.*, 2010; *Couvreux et al.*, 2011a;
140 2011b]. More recently, the 2014-2015 Green Ocean Amazon (GO-Amazon) campaign

141 [*Martin et al.*, 2016] sought to quantify the impact of atmospheric composition and
142 aerosols under clean and polluted conditions on cloud formation and radiation over the
143 Amazon basin, as well as on shallow to deep convection development [*Anber et al.*,
144 2015a; *Tang et al.*, 2016; *Giangrande et al.*, 2017].

145

146 The remainder of this review article is organized as follows. In sections 2-4, we introduce
147 some fundamental considerations of the climate system components necessary for
148 understanding tropical land-atmosphere interactions, including convection, clouds, and
149 rainfall (Section 2), surface turbulent fluxes (Section 3), and vegetation and ecosystem
150 processes (Section 4). We then synthesize prior work on tropical land-atmosphere
151 interactions from both local and non-local perspectives (Section 5). We close this review
152 (Section 6) by highlighting what we view as the outstanding issues, challenges, and
153 knowledge gaps for tropical land-atmosphere interactions. For example, we argue that
154 shallow cloud feedback and its impact on radiation has received too little attention
155 compared to precipitation feedback, in rainforests especially.

156 2   Convection, clouds, and rainfall in the Tropics

157 The net radiative heating of the atmosphere in the global tropics—arising from the top-
158 of-the-atmosphere imbalance of net incoming solar (shortwave) radiation exceeding
159 outgoing terrestrial (longwave) radiation—leads to one of the defining hallmarks of the
160 tropics, namely very high rain rates. This is not to say, of course, that rainfall in the
161 tropics is high everywhere or at all times, as climates within the tropics can be both wet
162 and dry. Indeed, many of earth's desert regions are found on the margins of the tropics,
163 and apart from deserts, parts of the tropics may experience very dry conditions
164 seasonally. In this review, we will exclude consideration of deserts and focus on the
165 humid tropics.

166

167 2.1   Shallow vs. deep convection

168 The distinction between shallow and deep convection remains imprecise, as these have
169 been regarded as both fundamentally distinct or as a continuum, in both observations and
170 model convection parameterizations [*Khairoutdinov and Randall*, 2006; *Bretherton and*

171 *Park*, 2009; *Park and Bretherton*, 2009; *Rio et al.*, 2009; *Wu et al.*, 2009; *Del Genio and*
172 *Wu*, 2010; *Hohenegger and Bretherton*, 2011; *Böing et al.*, 2012; *D'Andrea et al.*, 2014;
173 *Rochetin et al.*, 2014b]. We will loosely refer to shallow convection as convection
174 confined below the freezing level (typically less than 3km deep) and comprising non-
175 precipitating clouds small characteristic motion scales (typically less than a km in the
176 horizontal).
177
178 An important point is that shallow convection is frequently generated by thermals rooted
179 in the boundary layer and is thus ultimately related to surface sensible (H) and latent heat
180 (LE) flux and their partitioning [*Gentine et al.*, 2013a; 2013b; *de Arellano et al.*, 2014;
181 *Tawfik et al.*, 2014, 2015a,b]. Within the Amazon, shallow convection and associated
182 clouds frequently occur over the vegetated surface, while over cooler and more humid
183 river basins, shallow clouds are virtually absent [*Gentine et al.*, 2013a; *Rieck et al.*, 2014;
184 2015; see also Figure 1]. In addition, shallow convection is strongly influenced by the
185 diurnal cycle of surface radiation and surface turbulent heat fluxes [*Gentine et al.*, 2013a;
186 2013b; *de Arellano et al.*, 2014].
187
188 On the other hand, we use the term deep convection in association with deep,
189 precipitating clouds. Deep convection may be triggered by a suite of thermodynamic or
190 dynamic processes, including: boundary layer thermals [*D'Andrea et al.*, 2014; *Guillod et*
191 *al.*, 2014; *Rochetin et al.*, 2014a; 2014b; *Anber et al.*, 2015a], radiative destabilization
192 [*Anber et al.*, 2015b], cold pools (cold density currents due to rain evaporation that cools
193 the air within precipitating downdrafts) [*Engerer et al.*, 2008; *Del Genio and Wu*, 2010;
194 *Böing et al.*, 2012; *Feng et al.*, 2015; *Torri et al.*, 2015; *Gentine et al.*, 2016; *Heever*,
195 2016; *Drager and van den Heever*, 2017] forced vertical motions such as via mesoscale
196 and large-scale circulations [*Werth and Avissar*, 2002; *Roy et al.*, 2003] or propagating
197 tropical wave activity [*Kuang*, 2008; 2010]. As such, deep convection may be viewed as
198 less dependent on the surface state compared to shallow convection.
199
200 Over the central Amazon a large fraction of wet season precipitation occurs during the
201 nighttime (Figure 2). Moreover, during the daytime in both the dry and the wet seasons,

the diurnal cycle reflects not only locally surface-triggered deep convection [*Khairoutdinov and Randall*, 2006; *Ghate and Kollias*, 2016] but also propagating mesoscale convective systems and squall lines throughout the Amazon basin *[Greco et al.*, 1990; *Ghate and Kollias*, 2016; *Rickenbach et al.*, 2002]. However, during the dry season, precipitation occurs more frequently with the "popcorn type" deep convection that is more locally triggered and thus directly related to the state of the land surface [*Ghate and Kollias*, 2016] (see an example here https://youtu.be/c2-iquZziPU). While shallow convection does not produce much rainfall, it exerts significant influence on deep convection through its control on surface radiative fluxes and on transport of moisture into the lower troposphere. More discussion will be given in Section 4.2.

2.2   Considerations for modeling tropical clouds, convection, and rainfall

Current generation climate models struggle to represent both shallow and deep convection over continents and their transitions [*Guichard et al.*, 2004; *Bechtold et al.*, 2013; *Yin et al.*, 2013; *D'Andrea et al.*, 2014; *Couvreux et al.*, 2015], especially in the tropics, as they exhibit substantial errors in the phasing and intensity of both the diurnal and seasonal cycles of convection [*Bechtold et al.*, 2013], as well as biases in the climatological distribution of rainfall over land. For example, over the Amazon, many climate models underestimate surface precipitation, evapotranspiration, and specific humidity [*Yin et al.*, 2013], with the dry bias in moisture extending upwards into the lower free troposphere [*Lintner et al.*, 2017]. Such biases may reflect deficiencies or errors in how convection is represented in models [*Yano and Plant*, 2012; *Stevens and Bony*, 2013; *Bechtold et al.*, 2014]. Indeed, in current generation climate models, cloud processes occur at scales smaller than resolved grid-scale prognostic variables and therefore need to be parameterized, i.e. represented as a function of the resolved-scale variables. This is important as it means that climate models do not explicitly represent the small-scale convective physics of the climate system. Evaluation of model performance for the Central Amazon can be found in Adams et al. [2013, 2015, 2017].

Cloud resolving models (CRMs) that include explicit convection at scales of ~1km alleviate many of the biases evident in coarser-scale, parameterized convection climate

233 models, especially in terms of the diurnal cycle of convection or the sign and magnitude
234 of the feedbacks between deep convection and surface evaporative fraction [*Grabowski*
235 1999, *Taylor et al.*, 2013; *Anber et al.*, 2015a]. Nonetheless, due to convective wave
236 coupling in the Tropics, a simple prescription of lateral boundary conditions in small-
237 domain CRMs may be problematic, as the convective scales ultimately interact with and
238 are coupled to planetary scales. With a sufficiently large domain and fine enough
239 resolution, coupling between the convective scales and planetary scales may be explicitly
240 resolved, but simulations of this nature are likely to be computationally too expensive for
241 many applications. However, techniques exist to represent the effect of large-scale
242 dynamics on the convective scales, which, when combined with cloud resolving
243 simulations, yield powerful tools for understanding land-atmosphere interactions in the
244 tropics, as we elaborate further below.
245

246   3   Surface turbulent fluxes in the Tropics

247 A major component of land-atmosphere interactions considered is related to surface
248 turbulent fluxes and associated momentum, energy, water and trace gases exchanges
249 between the land surface and atmosphere [*Goulden et al.*, 2004; *Fisher et al.*, 2009;
250 *Restrepo-Coupe et al.*, 2013]. Surface turbulent flux measurements are usually obtained
251 from eddy-covariance methods, typically located above the canopy [*Baldocchi et al.*,
252 2001]. Observing turbulent fluxes is challenging in tropical environments given logistics,
253 cost, maintenance, and harsh environmental factors such as intense rainfall, high wind,
254 and relative humidity, which impact sensors [*Campos et al.*, 2009; *Da Rocha et al.*, 2009;
255 *Restrepo-Coupe et al.*, 2013; *Zahn et al.*, 2016; *Chor et al.*, 2017; *Gerken et al.*, 2017]. In
256 light of these challenges, it is perhaps not surprising that even the best estimates of
257 surface turbulent fluxes manifest large uncertainties [*Mueller et al.*, 2011].
258

259 Apart from site level measurements, which are limited to a small number of locations
260 around the tropics, remote sensing observations can provideindirect information about
261 surface turbulent fluxes and other relevant quantities over tropical land regions. Remote
262 sensing observations are useful for generalizing and comparing fluxes across the tropics,

263   even if they are not as direct as site level measurements. Yet, there are considerable

264   uncertainties in remote sensing and reanalysis estimates of rainfall [*Washington et al.*,

265   2013; *Levy et al.*, 2017], radiation [*Jimenez et al.*, 2011], and surface turbulent fluxes

266   [*Jung et a*l., 2009; *Alemohammad et al.*, 2016] and especially in terms of upscaling point

267   observations to larger areas as those measurements are fundamentally indirect.

268

269   While direct, satellite-based retrievals of carbon (e.g., gross primary production (GPP))

270   and water fluxes would be most suitable for the study of tropical land-atmosphere

271   interactions, such retrievals are beyond current remote sensing capabilities. However,

272   some recent work demonstrates that existing satellite observations, especially Solar-

273   Induced Fluorescence (SIF), may be leveraged to remotely assess surface turbulent fluxes

274   in the tropics. In contrast to the normalized difference vegetation index (NDVI) or many

275   other vegetation indices which are indirect byproducts of photosynthesis [*Morton et al.*,

276   2014], SIF (at the leaf scale) is directly related to the ecosystem-scale photosynthesis

277   rate, providing important information on the impact of stressors on photosynthesis and is

278   available from existing remote sensing platforms [*Frankenberg et al.*, 2011; *Joiner et al.*,

279   2011; *Frankenberg et al.*, 2012; *Joiner et al.*, 2013; *Frankenberg et al.*, 2014; *Guanter et*

280   *al.*, 2014; *Lee et al.*, 2015; *Duveiller and Cescatti*, 2016; *Liu et al.*, 2017; *Thum et al.*,

281   2017; *Alexander et al.*, 2017]. SIF is thus an important indicator of the rates of

282   photosynthesis and transpiration through stomatal (small pores at the leaf surface)

283   regulation [*Alemohammad et al.*, 2017; *Pagán et al.*, 2019]. Indeed, during

284   photosynthesis plants take up CO_2 from the atmosphere while releasing water to the

285   atmosphere through stomata. We note that recent developments in observations of SIF

286   seem to indicate that the major fraction of the SIF signal might be related to chlorophyll

287   photosynthetically active radiation and that changes in SIF yield (equivalent to light use

288   efficiency) may account for only a small fraction of the observed SIF signal [*Du et al.*,

289   2017]. This is still an open topic to better understand what is actually observed by SIF

290   remote sensing.

291

292   *Alemohammad et al.* [2016] applied a machine learning algorithm based on remotely-

293   sensed SIF, called WECANN (Water Energy and Carbon Artificial Neural Network) to

294   derive surface turbulent fluxes. WECANN reproduces exhibits reasonable interannual

295   variability and its seasonality is constrained by the use of SIF [*Alemohammad et al.*,

296   2016], yet like any other products it is not a direct observation of the fluxes, which are

297   only available at sparse tower observations. WECANN performs well compared to eddy-

298   covariance observations and has less uncertainty compared to many other retrievals (see

299   [*Alemohammad et al.*, 2017]).

300

301   Given the paucity of flux towers and associated surface flux measurements across the

302   tropics, we use WECANN to calculate surface flux climatologies across the continental

303   tropics. WECANN has been validated against available flux tower data and outperforms

304   other products in terms of reproducing both the seasonality and interannual variability

305   [*Alemohammad et al.*, 2017]. While remote sensing retrievals are not perfect and cannot

306   be considered the truth, they do provide spatially extensive data coverage, including

307   regions with sparse (or no) site-level measurements (e.g., Congo). In what follows, we

308   present climatologies of evapotranspiration (ET) and gross primary production (GPP) and

309   compare these against precipitation (based on GPCP 1DD v1.2 [*Huffman et al.*, 2001])

310   and net radiation (based on CERES SYN [*Kato et al.*, 2013]) in order to understand the

311   typical seasonal cycles of those energy, water, and carbon fluxes across the continental

312   tropics.

313

314   We first focus on the main tropical rainforests and the northeastern savanna (Cerrado)

315   region of Brazil (Figure 3). In the wetter part of the Amazon, net radiation, Rn, peaks in

316   the dry season (August to November) (Figure 3) when precipitation (Figure 4) and cloud

317   cover—especially shallow cloud cover, including fog—are reduced, [*Anber et al.*,

318   2015a]. As a result of reduced dry season cloud cover, incident surface solar radiation

319   increases, and both GPP (Figure 5) and ET (Figure 6) increase in the dry season (Figure

320   3). As discussed further in the next section, the forest in the climatologically wetter

321   Amazon is primarily light limited, while water stress there is moderate in the dry season.

322   The seasonal cycle is more pronounced for GPP than for ET (Figure 3): canopy

323   photosynthetic regeneration [*Lopez et al.*, 2016; *Saleska et al.*, 2003, 2006, 2016] is an

324   important factor affecting the seasonal cycle of GPP in rainforests potentially increasing

the maximum rate of GPP in the dry season. In addition, canopy evaporation (of intercepted rain) comprises a large fraction of total ET in the wet season [*Scott et al.*, 1997; *Oleson et al.*, 2008; *Miralles et al.*, 2010; *Sutanto et al.*, 2012; *van Dijk et al.*, 2015; *Andreasen et al.*, 2016] and partly compensates for reduced transpiration in the wet season. In fact, because of this compensation, the wettest parts of the Amazon exhibit weak ET seasonality. On the other hand, most land-surface models exaggerate water stress in the Amazon [*Powell et al.*, 2013], and typically exhibit much lower rates of ET and GPP in the dry season and simulate opposite seasonality of net ecosystem exchange compared to observations [*de Gonçalves et al.*, 2013; *Alemohammad et al.*, 2016; 2017]. This exaggerated water stress results from incorrect access to deep soil water, whether due to limited groundwater representation [*Maxwell and Condon,* 2016], because of the functional relationship of the water stress representation which does not obey physical constraints (such as flow down potential gradients as in plant hydraulics models) [*Kennedy et al.*, 2019] or simply because their assumed rooting depth is too shallow [*Fan et al.,* 2017].

In contrast to the everwet western and central Amazon, over the Cerrado region of Northeastern Brazil, the seasonal cycles of Rn, precipitation, GPP and ET are much more pronounced, with a marked dry season (Figure 3). The seasonal cycle of GPP tracks precipitation, and water stress, exhibiting a strong increase during the wet season. Similarly, ET increases sharply in the wet season and then decreases more slowly than precipitation in the dry region (Figure 3). Conversely, net radiation increases sharply during the dry season. This region clearly exhibits a strong water stress response.

Turning to the Maritime Continent, rainfall is intense throughout the year and seasonality is modest, with a short peak in November to January (Figure 3). Much of the seasonal cycle is attributable to monsoon circulations, which are strongly influenced by topography and the land- and ocean-surface thermal contrast [Chang 2005]. The topography and the distribution of island land masses leads to strong local variability (Figure 4e) and pronounced diurnal cycles in convection are evident [*Nitta*, 1987; *Hamada et al.*, 2008]. Additionally, the Madden Julian Oscillation, an important mode of

climate variability in the tropical Indo-Pacific with a lifecycle of 30-90 days, strongly impacts rainfall on intraseasonal timescales [*Hidayat and Kizu*, 2009]. Convective activity in the region also regulates the East Asian Monsoon [*Huang and Sun*, 1992]. The region is also influenced by topographic effects and land-see breeze interactions, which may impart considerable regional heterogeneity. Given the relatively constant regional-averaged precipitation with regular convection occurring over course of the annual cycle, ET and GPP remain near steady throughout the entire year in this mostly light limited environment (Figure 3).

The Congo basin exhibits two rainy seasons (Figure 3), with peaks in March-April-May and September-October-November, related to seasonal changes in moisture convergence associated with the African Easterly jet and Intertropical Convergence Zone (ITCZ) over the Atlantic [*Washington et al.*, 2013]. Throughout the year, monthly-mean precipitation is much less than that observed over the Amazon or Indonesia. The seasonality of GPP and, to a lesser extent, ET tracks that of precipitation, with substantial decreases during the June to August dry season and even more pronounced reduction during the December to February period. This seasonality in GPP and ET (Figure 3) suggests that the Congo basin should exhibit substantially more water stress during dry seasons compared to the Amazon or Indonesian rainforests [Guan et al. 2015].

Integrated over the entire tropical latitudinal band, precipitation is highest in DJF and MAM when the wet season extends over most of the Amazon and adjacent savanna regions (Figure 4). This seasonal cycle of tropical-mean precipitation largely determines the seasonal cycle of GPP. GPP peaks during the wet season in South America, as GPP is highest in the savanna regions while GPP over the rainforest exhibits less seasonal variations (Figure 6). The seasonal pattern of ET resembles GPP (Figure 6). Indeed, the seasonality in ET reflects the combined influences of 1) the seasonality of water availability in drier, water-limited regions, 2) the seasonality of surface radiation in the wetter, more energy-limited portion of the Amazon and 3) changes in photosynthetic capacity thoughout the year. The seasonal cycle of sensible heat flux (Figure 7) largely follows water stress, especially in the rainforest where radiation remains high throughout

387 the year, with an increase during the dry season. Water stress is further apparent in the

388 evaporative fraction, EF, the ratio of latent heat flux to the sum of latent and sensible heat

389 fluxes (Figure 8). Tropically-averaged EF does not evolve much over the year; the

390 modest seasonality may be understood in terms of variation of the latitudinal peak in

391 radiation and compensation of decreased canopy interception by transpiration (because of

392 increased net surface radiation) in the dry season. However, in transitional and dry

393 regions, EF exhibits much more seasonal variation. The surface moist static energy flux,

394 H+LE, shows some slight variations in SON and JJA but otherwise remains relatively

395 steady across longitudes because of the compensation between the increased H and

396 reduced ET in the dry season. In the dry to wet transition, SON, moist static energy flux

397 exhibits an interesting peak at about -60 longitude (Figure 9) through the combined

398 increase in radiation, due to reduced cloudiness, inducing higher sensible heat flux and

399 maintained high ET rates.

400

401 Over tropical Africa, the precipitation is highest in JJAS during the wet phase of the West

402 African Monsoon, with a secondary maximum in DJF corresponding to the Southern

403 African Monsoon (Figure 4). Similarly the latitudinal-averaged GPP and ET increase

404 during the West African Monsoon (Figure 5, Figure 6), accompanied by a strong

405 decrease in sensible heat flux (Figure 7). In DJF the southern African Monsoon displays

406 increased water flux (Figure 6) and photosynthesis tracking the increased rainfall (Figure

407 4). The Congo rainforest clearly exhibits two brief rainy seasons (Figure 3, Figure 8),

408 with peaks in March-April-May and September-October-November (Figure 3) and

409 displays substantial water stress and strong reduction in EF to values below 0.6 during

410 the dry season (Figure 8).

411

412 ## 4 Vegetation and ecosystem processes in the Tropics

413 We cannot understand tropical land-atmosphere interactions, not to mention the basic

414 features of terrestrial tropical climate, without consideration of vegetation and ecosystem

415 processes. Indeed, over land, what is viewed as the Tropics has traditionally been defined

416 with vegetation and ecosystems implicitly considered, as in the Köppen climate

417   classification scheme [Köppen, 1884]. Under this scheme, the terrestrial Tropics is

418   divided into three main *groups*—tropical rainforest, tropical monsoon, and tropical wet

419   and dry (or savanna)—all of which are characterized by annual mean temperatures

420   exceeding 18°C but which differ in terms of precipitation amount and seasonality.

421

422   One outstanding challenge in simulating tropical land regions is determining why most

423   contemporary land-surface models incorrectly represent the wettest rainforest GPP and

424   ET rates, their seasonal cycles, and how they relate to water stress? In the wettest tropical

425   forests, such as the western portion of the Amazon or Indonesia, energy and light limit

426   the rates of ET and GPP. It is thus reasonable to conclude that soil moisture and water

427   stress should have minor effects in such regions, and consequently, that precipitation

428   variability should not matter much. In fact, there exist sharp vertical gradients in the

429   canopy (as well as at the surface of the soil in the dry season) in terms of light and water

430   availability, along with nutrient allocation as well (Figure 10). Understory species receive

431   only a small amount of mostly diffuse light. However, water is typically not limiting for

432   low-canopy species, as relative humidity is high and VPD is low, leading to low stress on

433   understory conductance [*Leuning*, 1995; *Leuning et al.*, 1995; *Wang and Leuning*, 1998;

434   *Medlyn et al.*, 2011; 2012; *Heroult et al.*, 2013].

435

436   On the other hand, tall canopy species receive a large amount of radiation, especially in

437   the dry season, causing sunlit leaf warming and higher leaf VPD (e.g., Penman-Monteith

438   equation) that lead to heat and water stress [*Jardine et al.*, 2014]. Leaf and xylem water

439   status are regulated by the relative demand of sap from transpiration, which depends on

440   leaf VPD. It also depends on sap supply to the leaves, the rate of which is controlled by

441   the xylem conductivity and which is high for tall tropical rainforest trees [*Liu et al.,*

442   2019]. This conductivity is reduced by cavitation in the xylem (formulation of air bubbles

443   blocking the ascent of sap flow from the roots to the leaves) [*Martinez-Vilalta et al.*,

444   2014; *Martinez-Vilalta and Garcia-Forner*, 2016]. To avoid leaf desiccation and xylem

445   cavitation stomatal closure is usually observed during peak daytime sunlight hours in

446   rainforest top canopy species [*Brodribb*, 2003; *Pons and Welschen*, 2003; *Zhang et al.*,

447   2013]. This limits the risk of leaf desiccation or xylem cavitation (Figure 11), in those

448 usually efficient xylems. This type of behavior with strong stomatal regulation appears to
449 be typical in the tropical rainforests [*Fisher et al.*, 2006; *Konings and Gentine*, 2016],
450 even though this appears to contradict results from isotopic measurements showing that
451 stomata remain relatively open [*Ometto et al.,* 2006]. On seasonal time scales, this is
452 modulated by the change in photosynthetic capacity of the canopy due to leaf flush and
453 canopy regeneration [*Saleska et al.*, 2003, 2006]. More work is needed to understand
454 stomatal and canopy regulation of tropical rainforests in response to stressors, especially
455 given the importance of rainforests in the global carbon cycle.

456

457 In tall canopy species the flow in the xylem from the roots may be limited as the xylem
458 hydraulic conductivity is inversely proportional to height, though this is partially
459 compensated by a more efficient xylem (higher specific conductivity) [*Liu et al.,* 2019].
460 However, higher evaporative demand in the dry season and/or under anomalously dry
461 conditions can only be partially be mitigated by the more efficient xylem and by the plant
462 internal storage; stomatal shutdown may therefore be inevitable to avoid desiccation and
463 xylem cavitation (Figure 11) [Dawson, 1993; *Phillips et al.*, 1997; 2004; *Lee et al.*, 2005;
464 *Oliveira et al.*, 2005; *Phillips et al.*, 2008; *Scholz et al.*, 2011; *Zeppel et al.*, 2014;
465 *Konings and Gentine*, 2016]. In summary, water stress in tropical rainforest canopy
466 species may not primarily be due to soil water stress but rather to atmospheric demand or
467 a combination of soil moisture stress and atmospheric demand. The reduction of leaf and
468 xylem water potentials increase stress in the soil-plant continuum. Radiation, temperature
469 and VPD are therefore essential to understand tropical wet forests dryness response.

470

471 Land-surface and ecosystem models, apart from a few exceptions [*Xu et al.*, 2016;
472 *Kennedy et al., 2019*], do not represent plant hydraulics and typically only rely on an
473 empirical reduction of stomatal and ecosystem conductance, and therefore transpiration
474 and GPP, as functions of root-averaged soil moisture or water potential (e.g., [*Noilhan*
475 *and Planton*, 1989; *Sellers et al.*, 1996a; 1996b; *Ek*, 2003; *Boulet et al.*, 2007; *Gentine et*
476 *al.*, 2007; *Ngo-Duc et al.*, 2007; *Stoeckli et al.*, 2008; *Balsamo et al.*, 2009; *Boone et al.*,
477 2009a; *Bonan et al.*, 2011; *Lawrence et al.*, 2011; *Niu et al.*, 2011; *Bonan et al.*, 2012;
478 *Canal et al.*, 2014; *Han et al.*, 2014; *Naudts et al.*, 2014; *De Kauwe et al.*, 2015; *Chaney*

479 *et al.*, 2016; *Chen et al.*, 2016; *Haverd et al.*, 2016 among others). The root profile
480 averaging of soil moisture or water potential to define water stress exaggerates the impact
481 of surface drying, as in reality deeper roots may still effectively transport water to the
482 plant xylem even if surface roots experience dry conditions and therefore can maintain
483 overall high rates of GPP and transpiration.

484

485 The inclusion of plant hydraulics in tall canopy species leads to strong differentiation
486 between leaf (and upper xylem) and soil water potential (Figure 11) during midday,
487 especially in the dry season. Indeed, leaf and xylem water potentials substantially drop
488 because of the large transpiration rates through the stomata and because the xylem cannot
489 be instantaneously refilled due to the large flow drag in the elongated xylem. As a result,
490 plant hydraulics induce a shutdown of stomata during the day reducing the transpiration
491 rate near peak solar hours, also known as "midday depression," [*Malhi et al.,* 1998;
492 *Williams et al.,* 1998; *Harris et al*., 2004] in order to reduce desiccation of the leaf and
493 xylem. In addition, plant hydraulics also induces a natural hydraulic redistribution of
494 water in the root profile reducing dryness in the upper profile in the dry season [*Lee et*
495 *al.*, 2005; *Oliveira et al.*, 2005; *Domec et al.*, 2010; *Prieto and Ryel*, 2014; *Kennedy et*
496 *al., 2019*], using deep root moisture rather than surface soil moisture when needed, as the
497 water flows down gradient of water potentials. This is fundamentally different from
498 typical parameterizations using average water stress of the root water profile, which are
499 oversensitive to surface water stress, in typical parameterizations. Both of those effects
500 lead to reduced sensitivity to water stress and help maintain higher rates of transpiration
501 throughout the entire dry season, whereas typical land surface models overestimate water
502 stress in the dry season [*de Gonçalves et al.*, 2013; *Alemohammad et al.*, 2016; 2017].

503

504 ## 5 Tropical land-atmosphere interactions: Local and nonlocal
505 perspectives

506 Having reviewed some of the important components of tropical land-atmosphere
507 interactions, we now turn to the coupling of these components. Often, land-atmosphere
508 interactions are framed in terms of a one dimensional column, comprising a "point" of

509   interest, although a point here may be understood not only as a site (such as an eddy

510   covariance flux tower) but also as spatial averages of varying scales. While this local,

511   column view is certainly instructive, we suggest that it is also necessary to consider land-

512   atmosphere interactions through an interplay with remote influences, i.e., a nonlocal

513   perspective. This may be especially true in the tropics, given the strong coupling that

514   exists between convective and large-scales. We will revisit the seasonality of tropical

515   climate through the lens of these local and nonlocal perspectives of land-atmosphere

516   interactions.

517

518   ## 5.1   Quantifying land-atmosphere interactions

519   [*Green et al.*, 2017] recently developed a method to define the feedback between the

520   biosphere and atmosphere using multivariate conditional Granger causality (based on

521   lagged autoregressive vectors). We here use a similar framework using ET from

522   WECANN and precipitation from GPCP as well as photosynthetically active radiation

523   from CERES (Figure 12).

524

525   Most of the feedback between surface ET and precipitation occurs in the climatically

526   transitional and/or monsoonal regions, such as the savanna region of Northeastern Brazil

527   and the monsoonal regions over South Asia, the Sahel, Southern Africa, and Northern

528   Australia. In Brazil, these results are consistent with spatial transition inherent in the

529   convective margins concept introduced by Lintner and Neelin (2007; see also Figure 13)

530   and the impact of soil moisture and evapotranspiration on setting the location of the

531   transition between the dry and wet regions. The Sahelian and Southern African Monsoon

532   are also located in regions between very dry (deserts) and humid regions, where surface

533   feedback may be crucial for the penetration of the Monsoonal flow inland [*Lintner and*

534   *Neelin*, 2009; *Lintner et al.*, 2015]. Indeed, the biosphere in this region modulates the

535   local climate state: multiple equilibrium states, corresponding to different ecosystem

536   initial conditions, may exist under the same external (e.g., top of the atmosphere solar)

537   forcing [*Wang et al.*, 2000]. The effect of vegetation on land-atmosphere coupling

538   manifests itself at multiple timescales. At short timescales after precipitation, evaporation

539   is accelerated with intercepted water in the canopy. However, at longer timescales

540 vegetation acts to delay and prolong evaporation of water stored in the root zone. The
541 magnitude and timescale of these sources of water recycling vary depending on
542 ecosystem structure, including rooting depth and canopy structure, which may co-evolve
543 with atmospheric conditions at the interannual timescale [*Nicholson*, 2000]. This
544 represents a clear pathway for two-way feedbacks between the land surface and
545 precipitation.

546

547 We further emphasize that those feedbacks (Figure 12) are likely to also be influenced by
548 non-local conditions, with regional and large-scale changes in ocean to land flow and the
549 in-land distance of penetration influencing local coupling. We note that climate models
550 seem to exhibit soil moisture (and therefore evapotranspiration)- precipitation feedbacks
551 in similar tropical regions, when averaged across models, even though individual model
552 response varies [*Koster et al.*, 2011; *Seneviratne*, 2013] (one degree pixel and monthly
553 time scales). We emphasize that the PAR radiation product is very uncertain in the
554 tropics [*Jimenez et al.*, 2011] as it ultimately relies on a model to obtain surface incoming
555 radiation, which might explain the reduced biosphere-precipitation feedback strength in
556 the wet tropics compared to other regions. It is also likely that the bulk of the radiative
557 feedbacks are taking place at smaller times scales such as the ones observed with MODIS
558 (Figure 15). This shallow cloud cover is relatively steady spatially and in time, especially
559 in the dry season.

560

561   5.2   A local view of tropical land-atmosphere interactions

562 A critical aspect of land-atmosphere interactions in tropical rainforests is related to
563 shallow clouds and fog rather than deep convective clouds. Clearly, much of the focus of
564 tropical land-atmosphere interactions has been on feedbacks involving precipitating deep
565 convection, and the impact of surface heterogeneity on convective rainfall. On the other
566 hand, the coupling of the land surface to radiation has been relatively understudied.
567 Shallow clouds lead to reduced productivity and transpiration [*Anber et al.*, 2015a], yet
568 the latter depends on cloud thickness as cumulus clouds (shallow convection) generate
569 more diffuse light and may consequently boost photosynthesis when they are not too

570   thick [*Pedruzo-Bagazgoitia et al., 2017*], Figure 14. Fog on the other hand, strongly

571   diminishes the amount of incident light for ecosystems. Fog [*Anber et al.*, 2015a] and

572   shallow clouds [*Giangrande et al.*, 2017] appear to be two of the primary differences

573   between the dry and the wet season (in addition to the preferential occurrence of

574   nighttime mesoscale convective systems in the rainy season, which are not directly

575   relevant for land-atmosphere interactions associated with daytime processes). Low-level

576   cloudiness largely affects the surface incoming radiation by reducing shortwave surface

577   incoming radiation in the wet season, especially in the morning [*Anber et al.*, 2015a;

578   *Giangrande et al.*, 2017], which in turn leads to strong reduction in GPP and ET. These

579   clouds are also tightly connected to surface processes and especially the surface energy

580   partitioning. Indeed, nighttime fog, which often persists into the early daylight hours.

581   This fog is due to nighttime longwave cooling in very humid boundary layers, due for

582   instance to evening rain in the wet season [*Anber et al.*, 2015a]. Shallow clouds are

583   themselves directly forced by surface-generated thermals, i.e. boundary layer processes,

584   and they are modified by the sensible and latent heat flux magnitude [*de Arellano et al.*,

585   2014, 2019]. Shallow convection and low-cloud cover are also tightly connected to

586   ecosystem seasonality and to the diurnal cycle [*Anber et al.*, 2015a; *Tang et al.*, 2016;

587   *Giangrande et al.*, 2017].

588

589   Historically, the study of land-atmosphere interactions in the Tropics, and tropical

590   rainforests in particular, has emphasized effects of heterogeneity, especially due to

591   deforestation, on the generation of deep convection through mesoscale circulations (see

592   [*Lawrence and Vandecar*, 2015] for a complete review, as well as [*Avissar and Pielke*,

593   1989; *Pielke and Avissar*, 1990; *Pielke et al.*, 1991; *Dalu et al.*, 1996; *Avissar and*

594   *Schmidt*, 1998; *Taylor et al.*, 2007; 2009; 2011; *Rieck et al.*, 2015; *Khanna et al.*, 2017]).

595   The hypothesis behind this is that deforestation reduces EF and surface roughness

596   [*Khanna et al.*, 2017]. The associated increased buoyancy flux over the deforested areas,

597   mostly reflecting a shift toward increased sensible heating, induces mesoscale

598   circulations. These circulations enhance cloudiness through local buoyancy fluxes,

599   turbulent kinetic energy generation, and low-level moisture advection from adjacent

600   forested areas, thus providing all the key ingredients for moist convection generation

601 [*Rieck et al.*, 2014; 2015]. It seems unlikely however that momentum roughness plays a

602 major role in this high radiation environment [*Park et al.*, 2017], where circulations are

603 mostly buoyancy-driven. Instead, the heat and moisture roughness lengths [*Park et al.*,

604 2017] as well as leaf area index and stomatal conductance, which scales the magnitude of

605 the evapotranspiration flux, are the main players, in addition to changes in soil moisture

606 availability, for the circulation. The impact of the deforestation on surface fluxes and

607 local circulation can change from buoyancy-driven to surface roughness driven as the

608 spatial scale of the deforestation increases [Khanna et al 2017].

609

610 Induced mesoscale circulations and associated deep convection are clearly observable

611 with remote sensing observations [*Khanna et al.*, 2017] and are more important in the dry

612 season [*Khanna et al.*, 2017], when convection is more locally, and regionally, triggered

613 [*Anber et al.*, 2015a; *Ghate and Kollias*, 2016]. Once precipitation occurs, cold pools,

614 i.e., density currents induced by ice melt and evaporating rain in downdrafts, dominate

615 the surface-induced mesoscale circulation [*Rieck et al.*, 2015], and reduce the surface

616 heterogeneity signal. In the wet season, the relative contribution of local forcing to the

617 total rainfall is small as the bulk of the precipitation is due to mesoscale convective

618 systems or larger-scale systems propagating throughout the basin, less tightly connected

619 to surface and boundary layer processes [*Ghate and Kollias*, 2016].

620

621 Even during the dry season, a large fraction of the Amazon and of Indonesia only

622 experience minimal water stress (Figure 8 and Figure 7) so that increased radiation

623 generates higher rates of photosynthesis (Figure 5) and ET (Figure 6) [*Anber et al.*,

624 2015a]. Indeed, higher transpiration in the dry season (due to the higher demand which is

625 not entirely compensated by the slight water stress) can compensate the effect of reduced

626 rain reevaporation intercepted by the canopy. As a result the feedback loop between

627 precipitation and ET is weakened and the impact of the dry season on ET (and hence

628 clouds) is strongest (Figure 14). In addition, the feedback of shallower clouds and surface

629 radiation may be more important, Figure 14, than the feedback of deeper clouds and

630 precipitation, as those shallow clouds are preferentially triggered over drier surfaces.

631 Because shallow clouds have a small life cycle (typically less than 30 minutes) compared

632 to deep convective and mesoscale systems, they are more directly connected to the
633 underlying surface conditions and interact more with the local conditions.

634

635 Fewer studies have studied changes in shallow clouds [*Wang et al.*, 2000; *Lawton et al.*,
636 2001; *Chagnon et al.*, 2004; *Ray et al.*, 2006; *Wang et al.*, 2009; *Pielke et al.*, 2011; *Rieck*
637 *et al.*, 2014; *Anber et al.*, 2015a], even though the impact of changes in the surface
638 energy partitioning and heterogeneity on low-level clouds is clear and spatially
639 systematic (Figure 15). Given the importance of cloud cover on shortwave radiation and
640 their importance for the differentiation between the dry and wet seasons over wet tropical
641 rainforests we believe that this low-cloud feedback might be quite critical for rainforest
642 ecosystem functioning. Indeed it was pointed out by [*Morton et al.*, 2014; *Anber et al.*,
643 2015a; *Morton and Cook*, 2016] that light changes between the dry and wet season due to
644 changes in cloud cover were one of the primary reasons for changes in the seasonality of
645 surface fluxes, in addition to leaf flush out [*Lopes et al.*, 2016; *Saleska et al.*, 2016]. At
646 sub-daily scales, the shading due to low clouds reduces surface temperature and
647 ecosystem respiration [*Mahecha et al.*, 2010; *Peterhansel and Maurino*, 2011; *Thornley*,
648 2011; *Hadden and Grelle*, 2016; *Ballantyne et al.*, 2017]. This reduction depends
649 strongly on the cloud cycling and thickness. As a result, cloud-induced reductions in
650 respiration can cancel reductions in photosynthesis, such that the net effect of cloud
651 shading on net ecosystem exchange is unclear. *Horn et al.* [2015] showed that by
652 explicitly calculating the surface coupling leads to a change in the length scales of clouds,
653 and a reduction of the cloud life time. As a result, and although the cloud cover remains
654 almost the same there are larger populations of smaller shallow cumuli. This responses to
655 vegetation influence also the moisture transport and the cloud characteristics [*Sikma et al*,
656 2019].

657

658 In addition to regulating radiative energy balance at the surface, [*Wright et al.*, 2017]
659 have shown that shallow convection transports moisture, provided by plants'
660 transpiration, from the atmospheric boundary layer to the lower troposphere during the
661 late dry season and early dry to wet transition seasons (July-September) [*Fu and Li*,
662 2004]. This mechanism, referred to as the "shallow convective moisture pump", plays an

663 important role in priming the atmosphere for increasing deep convection (e.g., [*Schiro et*
664 *al.*, 2016; *Zhuang et al.*, 2017]), and wet season onset over the Amazon [*Wright et al.*,
665 2017].

666

667 The results discussed until now omitted the relation between physical processes and the
668 atmospheric composition, and more specifically the role of chemical reactions and
669 aerosols. Over rainforests, the pristine and undisturbed conditions of the atmospheric
670 boundary layer described in the seminal study by [*Garstang and Fitzjarrald*, 1999] are
671 currently undergoing rapid changes due to atmospheric composition modifications. Their
672 direct impact on the radiative and microphysical properties are due to biomass burning
673 and enhancement of concentrations of secondary organic aerosol precursors. Biomass
674 burning in Amazonia leads to increased aerosol optical depth and to abnormal
675 distributions of the heating rate profile. Analyzing systematic experiments performed by
676 large-eddy simulations, *Feingold et al.*, [2005] studied the processes that lead to the
677 suppression of clouds. Firstly, at the surface there are clear indications that the latent and
678 sensible heat flux are reduced, yielding convective boundary layers characterized by less
679 turbulent intensity and by delays in the morning transition [*Barbaro and Vilà-Guerau de*
680 *Arellano*, 2014]. Both aspects tend to reduce cloud formations. Secondly, [*Barbaro and*
681 *Vilà-Guerau de Arellano*, 2014] indicated that the vertical location of the smoke layer is
682 crucial in determining the dynamics of the boundary layer which can delay the onset of
683 shallow cumulus. In turn, and ass. As described by [*Feingold et al.*, 2005], smoke
684 confined in the well-mixed sub-cloud layer might positively benefit the cloud formation
685 since it distributes the heat uniformly that contributes to enhance convection. On the
686 other hand, smoke layers located within the cloud layer tend to stabilize the cloud layer
687 and therefore decrease the possibility of cloud formation. These results are very much
688 dependent on the aerosol optical properties defined by their heating, scattering and
689 hygroscopic properties. As a first indicative figure, the mentioned LES study and
690 observations by [*Koren et al.*, 2004] stressed that smoke layers with an aerosol optical
691 depth larger than 0.5 might already lead to cloud suppression by 50%. *Yu et al.* [2008]
692 have shown observationally that the influence of aerosols on shallow clouds varies with
693 meteorological conditions. When the ambient atmosphere is drier (relative humidity

694 ≤60%), cloud burning effect (evaporation of cloud droplets) due to increased absorption

695 of solar radiation by aerosols outweighs the increase of cloud droplets due to aerosol-

696 cloud microphysical effect. The reduced shallow clouds can further enhance the surface

697 dryness. In contrast, when the ambient atmosphere is relatively humid (relative humidity

698 ≥60%), the aerosol-cloud microphysical effect outweighs the cloud burning effect,

699 leading to an increase of shallow clouds and relative humidity near surface. In so doing,

700 aerosols can amplify the original moisture anomalies near the surface. Aerosols have also

701 shown to increase the lifetime of mesoscale convection over Congo and Amazon, due to

702 the delay of the precipitation that enhances ice formation and increased lifetime of the

703 mature and decay phase of deep convection [*Chakraborty et al.*, 2016].

704

705 These modifications are not only related to the direct emission of aerosol, but also to

706 changes in the gas phase chemistry that act as a precursor for the formation of secondary

707 organic aerosol. *Andreae et al.*, [2002] showed large differences in NO_x and ozone (O_3)

708 mixing ratio throughout the Amazon from rather pristine conditions with NO_x and ozone

709 levels below 0.1 ppb and 20 ppb, to values above 0.1 ppb and maximum levels of O_3 near

710 50 ppb near Manaus. Recent field experiments within the Green Ocean Amazon

711 campaign (GoAmazon) [*Fuentes et al* 2016; *Martin et al.*, 2016] corroborate these

712 levels as well as the high levels of the bio-organic compounds, in particular isoprene and

713 monoterpene. Closely related, these changes are accentuated by anthropogenic emissions,

714 from Manaus. The unique distribution of aerosols in Amazonia might explain observed

715 differences in deep convection, in particular lightning frequency, between Amazonia, the

716 Maritime continent and the Congo basin [Williams et al. 2004]. To represent these

717 chemistry changes and their effect on convection adequately, the dynamics that drive

718 processes such as the entrainment of pollutants from the free troposphere need to be taken

719 into account [Vila-Guerau de Arellano et al., 2011]. As a result of this interaction

720 between radiation, the land surface, dynamics and chemical processes, the frequency of

721 the clear convective vs. shallow cloudy conditions may be modified in the future. Current

722 efforts in monitoring them and improving the parameterizations of convection are under

723 way [Dias et al., 2014]. These efforts should include also in an integrated manner the

724 combined role of dynamics and chemistry to quantify relevant processes Two of them are

725 relevant and difficult to be represented in large-scale models. First, the role of canopy in
726 controlling the emission and deposition of the aerosol precursors on tropical rain forest
727 [*Freire et al*., 2017]. Second ventilation of pollutants from the sub-cloud layer into the
728 cloud layer, i.e. mass flux parameterizations, under representative Amazon conditions
729 [*Ouwersloot et al*., 2013].
730
731 In addition to affecting cloud microphysics, biomass burning in the tropics significantly
732 affects the global carbon budget. For example, in September and October of 2015 fires in
733 the Maritime continent released more terrestrial carbon (11.3 Tg C) than the
734 anthropogenic emissions of the EU (8.9 Tg C) [*Huijnen et al.*, 2016]. The extent of forest
735 fires in this region is tied to El Niño-induced drought conditions, and antecedent sea
736 surface temperature (SST) patterns are closely related to burned area at the global scale,
737 particularly in hotspots concentrated in the tropics [*Chen et al., 2016*]. Aerosol emissions
738 and biomass burning exert a strong control on land-atmosphere coupling of the carbon
739 and water cycles, and the consequences of this coupling is observable globally.
740
741   5.3   Nonlocal view of tropical land-atmosphere interactions
742   5.3.1   Moisture tracking and source attribution
743 A fundamental consideration in the study of the hydrologic cycle over tropical continents
744 is where the moisture for precipitation ultimately derives. In fact, many of the seminal
745 studies of tropical land region water cycle in the 1980s and 1990s focused on the concept
746 of recycling, i.e., the contribution of evapotranspiration over a region of interest to
747 precipitation in that region [*Salathi et al.* 1983, *Brubaker et al.* 1993; *Eltahir and Bras*,
748 1994; *Trenberth* 1999]. While these early studies typically estimated recycling used bulk
749 formulas derived under simplifying assumptions, more sophisticated approaches for
750 estimating recycling have emerged [*van der Ent et al* 2010, including comprehensive
751 moisture tracking operating on subdaily inputs on models and reanalysis, e.g., the
752 Dynamic Reycling Model [*Dominguez et al.* 2006], the Water Accounting Model (van
753 der Ent et al. 2010), and Lagrangian approaches using parcel dispersion models such as

754   Flexpart [*Gimeno et al.* 2012]. Contemporary estimates of recycling ratios for the

755   Amazon Basin range from 25%-35% [*Zemp et al.* 2014].

756   These more sophisticated approaches have also enabled identification and quantification

757   of upstream sources of moisture that lead to downstream rainfall over tropical land

758   regions [*Dirmeyer et al.,* 2007; *Drumond et al.,* 2014; *Hoyos et al.,* 2018; *Stohl and*

759   *James*, 2005]. For example, by combining a Lagrangian back trajectory approach with

760   rainfall and leaf area index data, [*Spracklen et al.*, 2012] quantified the linkage between

761   downstream rainfall amount and upstream air mass exposure to vegetation (Figure 17).

762   Over more than half of the tropical land surface, Spracklen et al. estimate a twofold

763   increase in downstream rainfall for those air masses passing over extensive vegetation

764   compared those passing over little upstream vegetation. Based on these estimates and

765   extrapolating current Amazonian deforestation trends into the future, these authors

766   project wet and dry season rainfall decreases of 12 and 21%, respectively, by the year

767   2050. In some regions, such attributions underscore the importance of upstream land

768   regions as moisture sources: for example, [*Drumond et al.*, 2014] used the FLEXPART

769   model forced with ERA-Interim reanalysis to estimate $E - P$ along trajectories passing

770   over the La Plata Basin in subtropical South America to establish that much of the

771   moisture entering this region derives from the Amazon Basin to the north and west.

772

773   5.3.2   Large-scale coupling, idealized modeling

774   Some studies have attempted to frame tropical land-atmosphere interactions in larger-

775   scale, and implicitly non-local, way [*Zeng and Neelin* 1999, *Lintner et al.* 2013; *Berg et*

776   *al.* 2017; *Langenbrunner et al.* 2019]. For example, Lintner et al. [2013] developed an

777   idealized prototype for diagnosing large-scale land-atmosphere coupling constructed

778   from coupling the vertically-integrated temperature and moisture equations to a simple

779   bucket soil moisture model. From this model, they derived analytic sensitivity of

780   precipitation to soil moisture spatial variation along a transect to various process

781   parameters related to convection and radiation, such as the timescale for convective

782   adjustment and the strength of cloud-radiative feedback. *Schäfli et al.*, [2012] developed

783   a conceptually similar model from which an analytic expression for the ratio of

784   evapotranspired moisture integrated along flow path to precipitation (or recycling ratio)

785 was obtained (Figure 16). Such idealized model frameworks, which consider tropical

786 land-atmosphere interactions by coupling both water and energy cycles, can be helpful in

787 interpreting and diagnosing linkages between local and non-local feedbacks.

788

789 5.4 Land-atmosphere interactions and their impact on tropical seasonality

790 One of the outstanding issues in the study of tropical land region climates involves

791 controls on precipitation seasonality, particularly its regional variability. Generally, the

792 seasonality follows the variation in maximum solar heating, but other factors, such as

793 ocean thermal inertia, topography, dynamics and circulation, and moisture transport, as

794 well as the state of the land surface, can exert considerable influence on the timing and

795 amplitude of tropical land region seasonal evolution. Over the Amazon basin, seasonality

796 exhibits marked variation in both latitude and longitude: for example, at 5S, the dry-to-

797 wet transition proceeds from the central Amazon eastward toward the Atlantic coast

798 [*Liebmann and Marengo*, 2001]. It is also worth noting a pervasive tendency for the dry-

799 to-wet season transition to occur much more rapidly than the wet-to-dry transition, as

800 evident in tropical monsoon systems including South Asia, West Africa, and South

801 America.

802

803 Analyzing multiple observational and reanalysis products, [*Fu and Li*, 2004] identified a

804 strong influence of surface turbulent fluxes on the dry-to-wet transition and its

805 interannual variability over the Amazon. In particular, their results link earlier wet

806 season onset to wetter conditions in the antecedent dry season: the higher latent fluxes at

807 the end of a wetter dry season encourage weaker convective inhibition (CIN) and

808 enhance CAPE, both of which are more favorable to wet season rainfall occurrence.

809 However, these authors also underscore the participation of the large-scale circulation

810 and its role in establishing a background environment (e.g., moisture convergence) to

811 support wet season rainfall. Incursion of cold fronts into the southern Amazon may act as

812 triggers for rapid initiation of wet season onset once the local thermodynamics become

813 favorable [*Li et al.*, 2006].

814

815 Recent research suggests that the land-atmosphere coupling is integral to the earlier
816 occurrence of determining earlier occurrence of wet season onset over western and
817 southern Amazonia, relative to that of eastern Amazonia. Both in situ and satellite
818 ecological observations have consistently shown that rainforests increase their
819 photosynthesis, and thus evapotranspiration (ET), during late dry season across
820 Amazonia (e.g., [*Huete et al.*, 2006; *Lopes et al.*, 2016; *Munger et al.*, 2016; *Wehr et al.*,
821 2016]). The wet season onset over the Southern Hemisphere portion of western
822 Amazonia occurs during September to October, about two to three months before the
823 Atlantic ITCZ [*Fu et al.*, 2016]. Using several satellite measurements, including the
824 isotopic signature of deuterium in atmospheric water vapor (HDO) and SIF, Wright et al.
825 [2017] have shown that increasing late dry season ET is the primary source of increasing
826 water vapor in the lower troposphere that initiates the increase of deep convection and
827 rainfall over southern Amazonia. In particular, the increase of water vapor with enriched
828 HDO in the boundary layer and free troposphere follows the increase of photosynthesis
829 during late dry season prior to wet season onset. During this period, the water vapor
830 HDO is too high to be explained by transport from Atlantic Ocean, and is consistent with
831 that from plant transpiration. Such a moistening of the atmosphere starts in western
832 southern Amazonia, the part of Amazonia that is most remote from the Atlantic Ocean
833 with high biomass. It then progresses towards eastern southern Amazonia. Thus, during
834 the late dry season this appears to contribute to the timing and spatial variation of the
835 initial moistening of the atmosphere, that ultimately lead to wet season onset over
836 southern Amazonia.

837

838 Wet season onset over southern Amazonia has been increasingly delayed since the late
839 1970s [*Marengo et al.*, 2011; *Fu et al.*, 2013]. In addition to the influence of global
840 circulation change, such a change has been attributed to land use. For example, [*Butt et
841 al.*, 2011] have compared long-term rainfall data between deforested and forested areas
842 over part of the southern Amazonia. They observed a significant delay in wet season
843 onset over the deforested areas, consistent with that implied by Wright et al. [2017]. In
844 addition, [*Zhang et al.*, 2008; 2009] have shown that biomass burning aerosols, which

845 peak in late dry season, can also weaken and delay dry to wet season transition by
846 stabilizing the atmosphere, reducing clouds and rainfall.

847   6   Discussion – conclusions

848 In this review paper, we have discussed some of the important aspects of land-
849 atmosphere interactions pertaining to the tropics. While our review is by no means
850 exhaustive, it illustrates some of the key processes in the coupled tropical land-
851 atmosphere system acting across multiple spatial and temporal scales, especially in
852 rainforest ecosystems.

853

854 We have argued that feedbacks between the land surface and precipitation in the tropics
855 are possibly non-local in nature (for instance due to the weak temperature gradient) and
856 may mostly impact moisture advection from the ocean and the position of deep
857 convection onset. Local rainfall feedback associated with mesoscale heterogeneities
858 appear to be rather small in magnitude, at least compared to the annual-mean rainfall, and
859 not sufficiently spatially systematic to truly affect ecosystem functioning.

860

861 Moreover, we contend that land surface-cloud feedbacks, especially those involving
862 shallow clouds and fog, are critical in terms of regulating light (direct and diffuse),
863 temperature, and water vapor deficit over tropical forest, but such feedbacks have
864 received relatively less attention. Remote sensing platforms provide useful information
865 for quantifying such feedbacks, but these need to be complemented by ground
866 measurements. Eddy-covariance measurements may prove difficult to use, as mesoscale
867 circulations alter the homogeneity assumption of eddy-covariance methods.

868

869 We have also discussed errors and biases in the representation of tropical continental
870 climates in current generation climate and Earth system models. Multi-model
871 assessments of soil moisture-precipitation feedback strength in ensembles of earth system
872 models such as [*Koster et al.*, 2004] manifest strong land-precipitation feedbacks in
873 similar transitional regions as the ones observed [*Green et al*., 2017], which seems to be
874 mostly related to modification of the moisture advection penetration distance from the

875 ocean rather than to local feedbacks. These feedbacks appear to be of relatively minor

876 importance in the core of tropical rainforests but are more critical for more marginal

877 rainfall regions (savanna). These regions are of critical importance for the terrestrial

878 global carbon cycle, providing the main terrestrial sink, but might be severely impacted

879 by climate change and droughts in particular [*Laan Luijkx et al.*, 2015]. Whether the

880 interannual variability in surface CO_2 flux in those regions is a zero-sum game with wet

881 years compensating dry years still is an open question especially in the context of rising

882 CO_2 concentration.

883

884 The core of rainforests seems to be more affected by radiation feedbacks at relatively

885 small spatial scales (~1km), which can be dramatically influenced by land cover and land

886 use change. Projected rates of future deforestation are poorly constrained, especially

887 regionally, though in recent years, the Congo and Indonesia have experienced increasing

888 deforestation while the deforestation rate in the Amazon has dropped.

889

890

891 **Acknowledgments.** PG acknowledges new investigator grant NNX14AI36G, DOE Early

892 Career grant DE-SC0014203, NSF CAREER and GoAmazon DE-SC0011094. BRL

893 acknowledges NSF-AGS-1505198. We would like to acknowledge high-performance

894 computing support from Yellowstone (ark:/85065/d7wd3xhc) provided by NCAR's

895 Computational and Information Systems Laboratory, sponsored by the National Science

896 Foundation.

897

898   REFERENCES

899

900   Acevedo, O. C., O. L. L. Moraes, R. da Silva, D. R. Fitzjarrald, R. K. Sakai, R. M.

901   Staebler, and M. J. Czikowsky, Inferring nocturnal surface fluxes from vertical

902   profiles of scalars in an Amazon pasture, *Global Change Biol*, *10*(5), 886–894,

903   doi:10.1111/j.1529-8817.2003.00755.x, 2004.

904   Alemohammad, S. H., B. Fang, A. G. Konings, F. Aires, J. K. Green, J. Kolassa, D.

905   Miralles, C. Prigent, and P. Gentine, Water, Energy, and Carbon with Artificial

906   Neural Networks (WECANN): a statistically based estimate of global surface

907   turbulent fluxes and gross primary productivity using solar-induced fluorescence,

908   *Biogeosciences*, *14*(18), 4101–4124, doi:10.5194/bg-14-4101-2017, 2017.

909   Alemohammad, S. H., B. Fang, A. G. Konings, J. K. Green, J. Kolassa, C. Prigent, F.

910   Aires, D. Miralles, and P. Gentine, Water, Energy, and Carbon with Artificial Neural

911   Networks (WECANN): A statistically-based estimate of global surface turbulent

912   fluxes using solar-induced fluorescence,, 1–36, doi:10.5194/bg-2016-495, 2016.

913   Alexander, J. N., J. R. Peter, and N. K. Ernest, Assimilating solar-induced chlorophyll

914   fluorescence into the terrestrial biosphere model BETHY-SCOPE: Model description

915   and information content, *geosci-model-dev-discuss.net*, doi:10.5194/gmd-2017-34,

916   2017.

917   Anber, U., P. Gentine, S. Wang, and A. H. Sobel, Fog and rain in the Amazon,

918   *Proceedings of the National Academy of Sciences*, *112*(37), 11473–11477,

919   doi:10.1073/pnas.1505077112, 2015.

920   Anber, U., S. Wang, and A. Sobel, Effect of Surface Fluxes versus Radiative Heating

921   on Tropical Deep Convection, *Journal of Atmospheric Sciences*, *72*(9), 3378–3388,

922   doi:10.1175/JAS-D-14-0253.1, 2015.

923   Andreae, M.O., Artaxo, P., Brandao, C., Carswell, F.E., Ciccioli, P., Da Costa, A.L.,

924   Culf, A.D., Esteves, J.L., Gash, J.H.C., Grace, J. and Kabat, P., Biogeochemical

cycling of carbon, water, energy, trace gases, and aerosols in Amazonia: The LBA-EUSTACH experiments, *J Geophys Res-Atmos*, *107*(D20), doi:10.1029/2001JD000524, 2002.

Andreasen, M., K. H. Jensen, D. Desilets, M. Zreda, H. Bogena, and M. C. Looms, Can canopy interception and biomass be inferred from cosmic-ray neutron intensity? Results from neutron transport modeling,, 1–42, doi:10.5194/hess-2016-226, 2016

Avissar, R., and C. Nobre, Preface to special issue on the Large-Scale Biosphere-Atmosphere Experiment in Amazonia (LBA), *J Geophys Res-Atmos*, *107*, –, doi:10.1029/2002JD002507, 2002

Avissar, R., and R. A. Pielke, A parameterization of heterogeneous land surfaces for atmospheric numerical models and its impact on regional meteorology, *Mon Wea Rev.*, 1989.

Avissar, R., and T. Schmidt, An evaluation of the scale at which ground-surface heat flux patchiness affects the convective boundary layer using large-eddy simulations, *J Atmos Sci*, *55*(16), 2666–2689, 1998.

Avissar, R., P. Dias, M. Dias, and C. Nobre, The Large-Scale Biosphere-atmosphere Experiment in Amazonia (LBA): Insights and future research needs, *J Geophys Res-Atmos*, *107*(D20), doi:10.1029/2002JD002704, 2002.

Baldocchi, D., Falge, E., Gu, L., Olson, R., Hollinger, D., Running, S., Anthoni, P., Bernhofer, C., Davis, K., Evans, R. and Fuentes, J.,FLUXNET: A new tool to study the temporal and spatial variability of ecosystem-scale carbon dioxide, water vapor, and energy flux densities, *Bull. Amer. Meteor. Soc.*, *82*(11), 2415–2434, 2001.

Ballantyne, A., Smith, W., Anderegg, W., Kauppi, P., Sarmiento, J., Tans, P., Shevliakova, E., Pan, Y., Poulter, B., Anav, A. and Friedlingstein, P., Accelerating net terrestrial carbon uptake during the warming hiatus due to reduced respiration, *Nature Climate Change*, *7*(2), 148–152, doi:10.1038/nclimate3204, 2017.

951   Balsamo, G., A. Beljaars, K. Scipal, P. Viterbo, B. van den Hurk, M. Hirschi, and A.

952   K. Betts, A Revised Hydrology for the ECMWF Model: Verification from Field Site

953   to Terrestrial Water Storage and Impact in the Integrated Forecast System, *J

954   Hydrometeorol*, *10*(3), 623–643, doi:10.1175/2008JHM1068.1, 2009.

955   Barbaro, E., and J. Arellano, Aerosols in the convective boundary layer: Shortwave

956   radiation effects on the coupled land-atmosphere system , *J of Climate*,

957   doi:10.1002/(ISSN)2169-8996., 2014

958   Bechtold, P., N. Semane, P. Lopez, J.-P. Chaboureau, A. Beljaars, and N. Bormann,

959   Representing equilibrium and non-equilibrium convection in large-scale models, *J

960   Atmos Sci*, *71*(2), 130919100122007–753, doi:10.1175/JAS-D-13-0163.1, 2013.

961   Bechtold, P., N. Semane, P. Lopez, J.-P. Chaboureau, A. Beljaars, and N. Bormann,

962   Representing Equilibrium and Nonequilibrium Convection in Large-Scale Models, *J

963   Atmos Sci*, *71*(2), 734–753, doi:10.1175/JAS-D-13-0163.1, 2014.

964   Berg, A.M, B.R. Lintner, K.L. Findell, and A. Giannini, (2017), Soil moisture

965   influence on seasonality and large-scale circulation in simulations of the West

966   African monsoon. *J. Clim.*, 30, 2295−2317, doi:10.1175/JCLI-D-0877.1.

967   Betts, A. K., and M. A. F. Silva Dias, Progress in understanding land-surface-

968   atmosphere coupling from LBA research, *J. Adv. Model. Earth Syst.*, *2*, 6,

969   doi:10.3894/JAMES.2010.2.6, 2010.

970   Betts, A. K., L. V. Gatti, and A. M. Cordova, Transport of ozone to the surface by

971   convective downdrafts at night, *J of Climate,* 2002.

972   Boisier, J. P., P. Ciais, A. Ducharne, and M. Guimberteau, Projected strengthening of

973   Amazonian dry season by constrained climate model simulations, *Nature Climate

974   Change*, *5*(7), 656–660, doi:10.1038/nclimate2658, 2015.

975 Bonan, G. B., K. W. Oleson, and R. A. Fisher, Reconciling leaf physiological traits
976 and canopy flux data: Use of the TRY and FLUXNET databases in the Community
977 Land Model version 4 , *J of Climate*, 2012.

978 Bonan, G. B., P. J. Lawrence, K. W. Oleson, S. Levis, M. Jung, M. Reichstein, D. M.
979 Lawrence, and S. C. Swenson, Improving canopy processes in the Community Land
980 Model version 4 (CLM4) using global flux fields empirically inferred from
981 FLUXNET data, *J Geophys Res-Biogeo*, *116*, 1–22, doi:10.1029/2010JG001593,
982 2011.

983 Boone, A., De Rosnay, P., Balsamo, G., Beljaars, A., Chopin, F., Decharme, B.,
984 Delire, C., Ducharne, A., Gascoin, S., Grippa, M. and Guichard, F., The AMMA
985 Land Surface Model Intercomparison Project (ALMIP), *Bull. Amer. Meteor. Soc.*,
986 *90*(12), 1865–1880, doi:10.1175/2009BAMS2786.1, 2009.

987 Boone, A., A. Getirana, J. Demarty, and B. Cappelaere, The African Monsoon
988 Multidisciplinary Analyses (AMMA) Land surface Model Intercomparison Project
989 Phase 2 (ALMIP2), *GEWEX News*, 2009

990 Boulet, G., A. Chehbouni, P. Gentine, B. Duchemin, J. Ezzahar, and R. Hadria,
991 Monitoring water stress using time series of observed to unstressed surface
992 temperature difference, *Agr Forest Meteorol*, *146*, 159–172,
993 doi:10.1016/j.agrformet.2007.05.012, 2007.

994 Böing, S. J., H. J. J. Jonker, A. P. Siebesma, and W. W. Grabowski, Influence of the
995 Subcloud Layer on the Development of a Deep Convective Ensemble, *J Atmos Sci*,
996 *69*(9), 2682–2698, doi:10.1175/JAS-D-11-0317.1, 2012.

997 Bretherton, C. S., and S. Park, A New Moist Turbulence Parameterization in the
998 Community Atmosphere Model, *J Climate*, *22*(12), 3422–3448,
999 doi:10.1175/2008JCLI2556.1, 2009.

Brodribb, T. J. Stomatal Closure during Leaf Dehydration, Correlation with Other Leaf Physiological Traits, *Plant Physiol*, *132*(4), 2166–2173, doi:10.1104/pp.103.023879, 2003.

Butt, N., P. A. de Oliveira, and M. H. Costa, Evidence that deforestation affects the onset of the rainy season in Rondonia, Brazil, *Journal of Geophysical Research: Atmospheres (1984–2012)*, *116*(D11), 407, doi:10.1029/2010JD015174, 2011.

Byrne, M. P., and P. A. O'Gorman, The Response of Precipitation Minus Evapotranspiration to Climate Warming: Why the "'Wet-Get-Wetter, Dry-Get-Drier'" Scaling Does Not Hold over Land, *J Climate*, doi:10.1175/JCLI-D-15-0369.s1, 2015.

Campos, J. G., O. C. Acevedo, J. Tota, and A. O. Manzi, On the temporal scale of the turbulent exchange of carbon dioxide and energy above a tropical rain forest in Amazonia, *J Geophys Res*, *114*(D8), D08124–10, doi:10.1029/2008JD011240., 2009

Canal, N., J. C. Calvet, B. Decharme, D. Carrer, S. Lafont, and G. Pigeon, Evaluation of root water uptake in the ISBA-A-gs land surface model using agricultural yield statistics over France, *Hydrol Earth Syst Sc*, *18*(12), 4979–4999, doi:10.5194/hess-18-4979-2014-supplement, 2014.

Chagnon, F. J. F., R. L. Bras, and J. Wang, Climatic shift in patterns of shallow clouds over the Amazon, *Geophys Res Lett*, *31*(24), L24212, doi:10.1029/2004GL021188, 2004.

Chaney, N. W., J. D. Herman, M. B. Ek, and E. F. Wood, Deriving Global Parameter Estimates for the Noah Land Surface Model using FLUXNET and Machine Learning, *J Geophys Res-Atmos*, 1–41, doi:10.1002/2016JD024821, 2016.

Chen, Y., Ryder, J., Bastrikov, V., McGrath, M.J., Naudts, K., Otto, J., Ottlé, C., Peylin, P., Polcher, J., Valade, A. and Black, A., Evaluating the performance of land surface model ORCHIDEE-CAN v1.0 on water and energy flux estimation with a

single- and multi-layer energy budget scheme, *Geosci Model Dev*, *9*(9), 2951–2972, doi:10.5194/gmd-9-2951-2016, 2016.

Chiang, J. C. H., & Sobel, A. H. (2002). Tropical tropospheric temperature variations caused by ENSO and their influence on the remote tropical climate. *Journal of Climate*, *15*(18), 2616–2631. https://doi.org/10.1175/1520-0442(2002)015<2616:TTTVCB>2.0.CO;2

Chor, T. L., N. L. Dias, A. Araújo, S. Wolff, E. Zahn, A. Manzi, I. Trebs, M. O. Sá, P. R. Teixeira, and M. Sörgel, Flux-variance and flux-gradient relationships in the roughness sublayer over the Amazon forest, *Agr Forest Meteorol*, *239*, 213–222, doi:10.1016/j.agrformet.2017.03.009, 2017.

Cook, B. I., S. P. Shukla, M. J. Puma, and L. S. Nazarenko, Irrigation as an historical climate forcing, *Climate dynamics*, *44*(5-6), 1715–1730, doi:10.1007/s00382-014-2204-7, 2014.

Couvreux, F., Roehrig, R., Rio, C., Lefebvre, M.P., Caian, M., Komori, T., Derbyshire, S., Guichard, F., Favot, F., D'Andrea, F. and Bechtold, P., Representation of daytime moist convection over the semi-arid Tropics by parametrizations used in climate and meteorological models, *Q J Roy Meteor Soc*, *141*(691), 2220–2236, doi:10.1002/qj.2517, 2015.

Couvreux, F., C. Rio, and F. Guichard, Initiation of daytime local convection in a semi-arid region analysed with high-resolution simulations and AMMA observations - *Quarterly Journal of the Royal Meteorological Society*, 2011

Couvreux, F., C. Rio, F. Guichard, M. Lothon, G. Canut, D. Bouniol, and A. Gounou, Initiation of daytime local convection in a semi-arid region analysed with high-resolution simulations and AMMA observations, *Q J Roy Meteor Soc*, *138*(662), 56–71, doi:10.1002/qj.903, 2011.

1052 Cox, P.M., Betts, R.A., Collins, M., Harris, P.P., Huntingford, C. and Jones, C.D.,
1053 2004. Amazonian forest dieback under climate-carbon cycle projections for the 21st
1054 century. *Theoretical and applied climatology*, *78*(1-3), 137-156.

1055 Da Rocha, H. R. et al., Patterns of water and heat flux across a biome gradient from
1056 tropical forest to savanna in Brazil, *J Geophys Res*, *114*, G00B12,
1057 doi:10.1029/2007JG000640, 2009.

1058 Daleu, C. L., S. J. Woolnough, and R. S. Plant (2012), Cloud-Resolving Model
1059 Simulations with One- and Two-Way Couplings via the Weak Temperature Gradient
1060 Approximation, *J Atmos Sci*, *69*(12), 3683–3699, doi:10.1175/JAS-D-12-058.1.

1061 Daleu, C. L., S. J. Woolnough, and R. S. Plant, Transition from suppressed to active
1062 convection modulated by a weak-temperature gradient derived large-scale circulation,
1063 *J Atmos Sci*, 141023140130007, doi:10.1175/JAS-D-14-0041.1, 2014.

1064 Dalu, G. A., R. A. Pielke, M. Baldi, and X. Zeng, Heat and momentum fluxes
1065 induced by thermal inhomogeneities with and without large-scale flow, *Journal of the*
1066 *atmospheric Science,* 1996.

1067 Davidson, E.A., de Araújo, A.C., Artaxo, P., Balch, J.K., Brown, I.F., Bustamante,
1068 M.M., Coe, M.T., DeFries, R.S., Keller, M., Longo, M. and Munger, J.W., The
1069 Amazon basin in transition, *Nature*, *481*(7381), 321–328, doi:10.1038/nature10717,
1070 2012

1071 Dawson, T. E. (1993). Hydraulic lift and water use by plants - implications for water
1072 balance, performance and plant-plant interactions. *Oecologia (Berl)*, *95*(4), 565–574

1073 de Arellano, J. V.-G., H. G. Ouwersloot, D. Baldocchi, and C. M. J. Jacobs, Shallow
1074 cumulus rooted in photosynthesis, *Geophys Res Lett*, doi:10.1002/2014GL059279,
1075 2014.

1076 De Kauwe, M. G., J. Kala, Y. S. Lin, A. J. Pitman, B. E. Medlyn, R. A. Duursma, G.
1077 Abramowitz, Y. P. Wang, and D. G. Miralles, A test of an optimal stomatal

1078   conductance scheme within the CABLE land surface model, *Geosci Model Dev*, *8*(2),
1079   431–452, doi:10.5194/gmd-8-431-2015, 2015.

1080   Del Genio, A. D., and J. Wu, The Role of Entrainment in the Diurnal Cycle of
1081   Continental Convection, *J Climate*, *23*(10), 2722–2738,
1082   doi:10.1175/2009JCLI3340.1, 2010.

1083   Dirmeyer, P., 2011: The terrestrial segment of soil moisture-climate coupling. *Geo*
1084   *Res Letters*, 38, L16702, doi:10.1029/2011GL048268, 2011, L16702

1085   Dirmeyer, Paul A., and Kaye L. Brubaker, 2007: Characterization of the global
1086   hydrologic cycle from a back-trajectory analysis of atmospheric water vapor. *Journal*
1087   *of Hydrometeorology* 8.1 (2007): 20-37.

1088   Domec, J.-C., J. S. King, A. Noormets, E. Treasure, M. J. Gavazzi, G. Sun, and S. G.
1089   McNulty, (2010), Hydraulic redistribution of soil water by roots affects whole-stand
1090   evapotranspiration and net ecosystem carbon exchange, *New Phytologist*, *187*(1),
1091   171–183, doi:10.1111/j.1469-8137.2010.03245.x,

1092   Dominguez, F., P. Kumar, X. Liang, and M. Ting, (2006) Impact of atmospheric
1093   moisture storage on precipitation recycling. *J. Climate*, 19, 1513–1530.

1094   Doughty, C.E., Metcalfe, D.B., Girardin, C.A.J., Amézquita, F.F., Cabrera, D.G.,
1095   Huasco, W.H., Silva-Espejo, J.E., Araujo-Murakami, A., Da Costa, M.C., Rocha, W.
1096   and Feldpausch, T.R., Drought impact on forest carbon dynamics and fluxes in
1097   Amazonia, *Nature*, *519*(7541), 78–82, doi:10.1038/nature14213, 2015.

1098   Drager, A. J., and S. C. van den Heever, Characterizing convective cold pools, *J. Adv.*
1099   *Model. Earth Syst.*, 1–55, doi:10.1002/2016MS000788, 2017.

1100   Drumond, A., J. Marengo, T. Ambrizzi, R. Nieto, L. Moreira, and L. Gimeno, The
1101   role of the Amazon Basin moisture in the atmospheric branch of the hydrological
1102   cycle: a Lagrangian analysis, *Hydrol Earth Syst Sc*, *18*(7), 2577–2598,
1103   doi:10.5194/hess-18-2577-2014, 2014.

Du, S., L. Liu, X. Liu, and J. Hu, Response of Canopy Solar-Induced Chlorophyll Fluorescence to the Absorbed Photosynthetically Active Radiation Absorbed by Chlorophyll, *Remote Sensing*, *9*(9), 911–19, doi:10.3390/rs9090911, 2017.

Duveiller, G., and A. Cescatti, Spatially downscaling sun-induced chlorophyll fluorescence leads to an improved temporal correlation with gross primary productivity, *Remote Sensing of Environment*, *182*(C), 72–89, doi:10.1016/j.rse.2016.04.027, 2016.

D'Andrea, F., P. Gentine, and A. K. Betts, Triggering deep convection with a probabilistic plume model, *J Atmos Sci*, *71*(11), 3881–3901, doi:10.1175/JAS-D-13-0340.1, 2014.

Ek, M. B., Implementation of Noah land surface model advances in the National Centers for Environmental Prediction operational mesoscale Eta model, *J Geophys Res*, *108*(D22), 8851, doi:10.1029/2002JD003296, 2003.

Eltahir, E.A.B., and R.L. Bras (1994): Precipitation Recycling in the Amazon Basin. *Quarterly Journal of the Royal Meteorological Society*, 120: 861-880

Engerer, N. A., D. J. Stensrud, and M. C. Coniglio, Surface Characteristics of Observed Cold Pools, *Mon Wea Rev*, *136*(12), 4839–4849, doi:10.1175/2008MWR2528.1, 2008.

Fan, Y., Miguez-Macho, G., Jobbágy, E. G., Jackson, R. B., & Otero-Casal, C. (2017). Hydrologic regulation of plant rooting depth. *Proceedings of the National Academy of Sciences*, *114*(40), 10572-10577.

Feingold, G., H. L. Jiang, and J. Y. Harrington, On smoke suppression of clouds in Amazonia, *Geophys Res Lett*, *32*(2), doi:10.1029/2004GL021369, 2005.

Feng, Z., S. Hagos, A. K. Rowe, C. D. Burleyson, M. N. Martini, and S. P. de Szoeke, Mechanisms of convective cloud organization by cold pools over tropical warm ocean during the AMIE/DYNAMO field campaign, *J. Adv. Model. Earth Syst.*, *7*(2), 357–381, doi:10.1002/2014MS000384, 2015.

1131   Fisher, J.B., Malhi, Y., Bonal, D., Da Rocha, H.R., De Araujo, A.C., Gamo, M.,
1132   Goulden, M.L., Hirano, T., Huete, A.R., Kondo, H. and Kumagai, T.O., The land-
1133   atmosphere water flux in the tropics, *Global Change Biol*, *15*(11), 2694–2714,
1134   doi:10.1111/j.1365-2486.2008.01813.x, 2009.

1135   Fisher, R. A., M. Williams, R. L. Do Vale, A. L. Da Costa, and P. Meir, Evidence
1136   from Amazonian forests is consistent with isohydric control of leaf water potential,
1137   *Plant Cell Environ*, *29*(2), 151–165, 2006.

1138   Fitzjarrald, D. R., Turbulent trasnport just above the Amazon, *J Geophys Res-Atmos*,
1139   1–13, 2007.

1140   Frankenberg, C., Fisher, J.B., Worden, J., Badgley, G., Saatchi, S.S., Lee, J.E., Toon,
1141   G.C., Butz, A., Jung, M., Kuze, A. and Yokota, T., New global observations of the
1142   terrestrial carbon cycle from GOSAT: Patterns of plant fluorescence with gross
1143   primary productivity, *Geophys Res Lett*, *38*(17), n/a–n/a,
1144   doi:10.1029/2011GL048738, 2011.

1145   Frankenberg, C., C. O'Dell, J. Berry, L. Guanter, J. Joiner, P. Köhler, R. Pollock, and
1146   T. E. Taylor, Prospects for chlorophyll fluorescence remote sensing from the Orbiting
1147   Carbon Observatory-2, *Remote Sensing of Environment*, *147*(C), 1–12,
1148   doi:10.1016/j.rse.2014.02.007, 2014.

1149   Frankenberg, C., C. O'Dell, L. Guanter, and J. McDuffie, Remote sensing of near-
1150   infrared chlorophyll fluorescence from space in scattering atmospheres: implications
1151   for its retrieval and interferences with atmospheric CO_2 retrievals, *Atmos Meas Tech*,
1152   *5*(8), 2081–2094, doi:10.5194/amt-5-2081-2012, 2012.

1153   Fu, R., and W. Li, The influence of the land surface on the transition from dry to wet
1154   season in Amazonia, *Theor Appl Climatol*, *78*(1-3), 97–110, doi:10.1007/s00704-004-
1155   0046-7., 2004

1156   Fu, R., L. Yin, W. Li, and P. A. Arias, Increased dry-season length over southern
1157   Amazonia in recent decades and its implication for future climate projection, 2013.

Fu, R., P. A. Arias, and H. Wang, The Connection Between the North and South American Monsoons, *The Monsoons and Climate Change*, 2016

Garstang, M., and D. R. Fitzjarrald, *Observations of surface to atmosphere interactions in the tropics.*, 1999

Gatti, L.V., Gloor, M., Miller, J.B., Doughty, C.E., Malhi, Y., Domingues, L.G., Basso, L.S., Martinewski, A., Correia, C.S.C., Borges, V.F. and Freitas, S., Drought sensitivity of Amazonian carbon balance revealed by atmospheric measurements, *Nature*, *506*(7486), 76–80, doi:10.1038/nature12957, 2015.

Gentine, P., A. Garelli, S. B. Park, and J. Nie, Role of surface heat fluxes underneath cold pools, *Geo Res Letters*, *43*(2), 874–883, doi:10.1002/2015GL067262, 2016.

Gentine, P., A. Holtslag, and F. D'Andrea, Surface and atmospheric controls on the onset of moist convection over land, *J Hydrometeorol*, *14*(5), 1443–1462, doi:10.1175/JHM-D-12-0137.1, 2013.

Gentine, P., C. R. Ferguson, and A. A. M. Holtslag, Diagnosing evaporative fraction over land from boundary-layer clouds, *J Geophys Res-Atmos*, *118*(15), 8185–8196, doi:10.1002/jgrd.50416, 2013.

Gentine, P., D. Entekhabi, A. Chehbouni, G. Boulet, and B. Duchemin, Analysis of evaporative fraction diurnal behaviour, *Agr Forest Meteorol*, *143*, 13–29, doi:10.1016/j.agrformet.2006.11.002, 2007.

Gerken, T., Ruddell, B.L., Fuentes, J.D., Araújo, A., Brunsell, N.A., Maia, J., Manzi, A., Mercer, J., dos Santos, R.N., von Randow, C. and Stoy, P.C.,, Investigating the mechanisms responsible for the lack of surface energy balance closure in a central Amazonian tropical rainforest, *Agr Forest Meteorol*, 1–0, doi:10.1016/j.agrformet.2017.03.023, 2017.

Ghate, V. P., and P. Kollias, On the controls of daytime precipitation in the Amazonian dry season, *J Hydrometeorol*, JHM–D–16–0101.1–55, doi:10.1175/JHM-D-16-0101.1, 2016.

1185   Giangrande, S. E. et al., Cloud Characteristics, Thermodynamic Controls and
1186   Radiative Impacts During the Observations and Modeling of the Green Ocean
1187   Amazon (GoAmazon2014/5) Experiment, *Atmos. Chem. Phys. Discuss.*, 1–41,
1188   doi:10.5194/acp-2017-452, 2017.

1189   Gimeno, L., and Coauthors, (2012), Oceanic and terrestrial sources of continental
1190   precipitation. *Rev. Geophys.*, 50, doi:https://doi.org/10.1029/2012RG000389.

1191   Goulden, M. L., S. D. Miller, and H. R. da Rocha, Diel and seasonal patterns of
1192   tropical forest CO2 exchange, *Ecological , 2004*

1193   Green, J. K., A. G. Konings, S. H. Alemohammad, J. Berry, D. Entekhabi, J. Kolassa,
1194   J.-E. Lee, and P. Gentine, Regionally strong feedbacks between the atmosphere and
1195   terrestrial biosphere, *Nat Geosci*, *48*, 1–12, doi:10.1038/ngeo2957, 2017.

1196   Green, J., Seneviratne, S. I., Berg, A. A., Findell, K. L., Hagemann, S., Lawrence, D.
1197   M., & Gentine, Pierre. (2019). Large influence of soil moisture on long-term
1198   terrestrial carbon uptake. *Nature*, *565*(7740), 476.
1199

1200   Greve, P., B. Orlowsky, B. Mueller, J. Sheffield, M. Reichstein, and S. I. Seneviratne,
1201   Global assessment of trends in wetting and drying over land, *Nat Geosci*, *7*(10), 716–
1202   721, doi:10.1038/ngeo2247, 2014.

1203   Guanter, L., Zhang, Y., Jung, M., Joiner, J., Voigt, M., Berry, J.A., Frankenberg, C.,
1204   Huete, A.R., Zarco-Tejada, P., Lee, J.E. and Moran, Global and time-resolved
1205   monitoring of crop photosynthesis with chlorophyll fluorescence, *PNAS*, *111*(14),
1206   E1327–E1333, doi:10.1073/pnas.1320008111, 2014.

1207   Guichard, F., Petch, J.C., Redelsperger, J.L., Bechtold, P., Chaboureau, J.P., Cheinet,
1208   S., Grabowski, W., Grenier, H., Jones, C.G., Köhler, M. and Piriou, J.M., Modelling
1209   the diurnal cycle of deep precipitating convection over land with cloud-resolving
1210   models and single-column models, *Q J Roy Meteor Soc*, *130*(604), 3139–3172,
1211   doi:10.1256/qj.03.145, 2004.

1212   Guillod, B.P., Orlowsky, B., Miralles, D., Teuling, A.J., Blanken, P.D., Buchmann,
1213   N., Ciais, P., Ek, M., Findell, K.L., Gentine, P. and Lintner, B.R., Land-surface
1214   controls on afternoon precipitation diagnosed from observational data: uncertainties
1215   and confounding factors, *Atmos. Chem. Phys*, *14*(16), 8343–8367, doi:10.5194/acp-
1216   14-8343-2014-supplement, 2014.

1217   Guillod, B. P., B. Orlowsky, D. G. Miralles, A. J. Teuling, and S. I. Seneviratne,
1218   Reconciling spatial and temporal soil moisture effects on afternoon rainfall, *Nat*
1219   *Comms*, *6*, 6443, doi:10.1038/ncomms7443, 2015.

1220   Ouwersloot H.G. , M. Sikma, C. M. J. Jacobs, J. V.-G. de Arellano, X. Pedruzo-
1221   Bagazgoitia, M. Sikma, and C. C. van Heerwaarden, Direct and Diffuse Radiation in
1222   the Shallow Cumulus–Vegetation System: Enhanced and Decreased
1223   Evapotranspiration Regimes, *J Hydrometeorol*, *18*(6), 1731–1748, doi:10.1175/JHM-
1224   D-16-0279.1, 2017.

1225   Hadden, D., and A. Grelle, Changing temperature response of respiration turns boreal
1226   forest from carbon sink into carbon source, *Agr Forest Meteorol*, *223*, 30–38,
1227   doi:10.1016/j.agrformet.2016.03.020, 2016.

1228   Hamada, J.-I., M. D. Yamanaka, S. Mori, Y. I. Tauhid, and T. Sribimawati,
1229   Differences of Rainfall Characteristics between Coastal and Interior Areas of Central
1230   Western Sumatera, Indonesia, *Journal of the Meteorological Society of Japan. Ser. II*,
1231   *86*(5), 593–611, doi:10.2151/jmsj.86.593, 2008.

1232   Han, X., H.-J. H. Franssen, C. Montzka, and H. Vereecken, Soil moisture and soil
1233   properties estimation in the Community Land Model with synthetic brightness
1234   temperature observations, *Water resources Research*, n/a–n/a,
1235   doi:10.1002/2013WR014586, 2014.

1236   Harris P. P., C. Huntingford, P. M. Cox, J. H. C. Gash, Y. Malhi, Effect of soil
1237   moisture on canopy conductance of Amazonian rainforest. Agricultural and Forest
1238   Meteorology 122, 215-227 (2004); published online EpubApr 20
1239   (10.1016/j.agrformet.2003.09.006).

1240   Haverd, V., M. Cuntz, L. P. Nieradzik, and I. N. Harman, Improved representations
1241   of coupled soil-canopy processes in the CABLE land surface model, *Geosci. Model*
1242   *Dev. Discuss.*, 1–24, doi:10.5194/gmd-2016-37, 2016.

1243   Grant, L. D., & van den Heever, S. C., Cold pool dissipation. *Journal of Geophysical*
1244   *Research: Atmospheres*, *121*(3), 1138-1155, 2016.

1245   Heroult, A., Y. LIN, and A. Bourne, Optimal stomatal conductance in relation to
1246   photosynthesis in climatically contrasting Eucalyptus species under drought, *Plant*
1247   *Cell and Env*, doi:10.1111/j.1365-3040.2012.02570.x, 2013.

1248   Hidayat, R., and S. Kizu, Influence of the Madden-Julian Oscillation on Indonesian
1249   rainfall variability in austral summer, *Int J Climatol*, *23*(12), n/a–n/a,
1250   doi:10.1002/joc.2005, 2009.

1251   Hilker, T., A. I. Lyapustin, C. J. Tucker, F. G. Hall, R. B. Myneni, Y. Wang, J. Bi, Y.
1252   Mendes de Moura, and P. J. Sellers, Vegetation dynamics and rainfall sensitivity of
1253   the Amazon, *Proceedings of the National Academy of Sciences*, *111*(45), 16041–
1254   16046, doi:10.1073/pnas.1404870111, 2014.

1255   Hohenegger, C., and C. S. Bretherton, Simulating deep convection with a shallow
1256   convection scheme, *Atmos. Chem. Phys*, *11*(20), 10389–10406, doi:10.5194/acp-11-
1257   10389-2011, 2011.

1258   Horn, G. L., H. G. Ouwersloot, J. V.-G. de Arellano, and M. Sikma, Cloud Shading
1259   Effects on Characteristic Boundary-Layer Length Scales, *Bound-Lay Meteorol*,
1260   *157*(2), 237–263, doi:10.1007/s10546-015-0054-4, 2015.

1261   Hoyos, I., Dominguez, F., Cañón-Barriga, J., Martínez, J. A., Nieto, R., Gimeno, L.,
1262   & Dirmeyer, P. A. (2018). Moisture origin and transport processes in Colombia,
1263   northern South America. *Climate dynamics*, *50*(3-4), 971-990.

1264

1265   Huang, R., and F. Sun, Impacts of the Tropical Western Pacific on the East Asian
1266   Summer Monsoon, *Journal of the Meteorological Society of Japan. Ser. II*, *70*(1B),
1267   243–256, doi:10.2151/jmsj1965.70.1B_243, 1992.

1268   Huete, A. R., K. Didan, Y. E. Shimabukuro, P. Ratana, S. R. Saleska, L. R. Hutyra,
1269   W. Yang, R. R. Nemani, and R. Myneni (2006), Amazon rainforests green-up with
1270   sunlight in dry season, *Geophys Res Lett*, *33*(6), L06405,
1271   doi:10.1029/2005GL025583, 2006.

1272   Huffman, G. J., R. F. Adler, M. M. Morrissey, D. T. Bolvin, S. Curtis, R. Joyce, B.
1273   McGavock, and J. Susskind, Global precipitation at one-degree daily resolution from
1274   multisatellite observations, *J Hydrometeorol*, *2*(1), 36–50, doi:10.1175/1525-
1275   7541(2001)002<0036:GPAODD>2.0.CO;2, 2001.

1276   Huijnen, V., M. J. Wooster, J. W. Kaiser, D. L. A. Gaveau, J. Flemming, M.
1277   Parrington, A. Inness, D. Murdiyarso, B. Main, and M. van Weele, Fire carbon
1278   emissions over maritime southeast Asia in 2015 largest since 1997, *Sci. Rep.*, 1–8,
1279   doi:10.1038/srep26886, 2016.

1280   Jardine, K., Chambers, J., Alves, E.G., Teixeira, A., Garcia, S., Holm, J., Higuchi, N.,
1281   Manzi, A., Abrell, L., Fuentes, J.D. and Nielsen, L.K., Dynamic Balancing of
1282   Isoprene Carbon Sources Reflects Photosynthetic and Photorespiratory Responses to
1283   Temperature Stress, *Plant Physiol*, *166*(4), 2051–2064, doi:10.1104/pp.114.247494,
1284   2014.

1285   Jimenez, C., Prigent, C., Mueller, B., Seneviratne, S.I., McCabe, M.F., Wood, E.F.,
1286   Rossow, W.B., Balsamo, G., Betts, A.K., Dirmeyer, P.A. and Fisher, J.B., Global
1287   intercomparison of 12 land surface heat flux estimates, *J Geophys Res*, *116*(D2),
1288   1147–27, doi:10.1029/2010JD014545, 2011.

1289   Joiner, J., A. P. Vasilkov, Y. Yoshida, L. A. Corp, and E. M. Middleton, First
1290   observations of global and seasonal terrestrial chlorophyll fluorescence from space,
1291   *Biogeosciences*, *8*(3), 637–651, doi:10.5194/bg-8-637-2011, 2011.

Joiner, J., L. Guanter, R. Lindstrot, M. Voigt, A. P. Vasilkov, E. M. Middleton, K. F. Huemmrich, Y. Yoshida, and C. Frankenberg, Global monitoring of terrestrial chlorophyll fluorescence from moderate-spectral-resolution near-infrared satellite measurements: methodology, simulations, and application to GOME-2, *Atmos Meas Tech*, *6*(10), 2803–2823, doi:10.5194/amt-6-2803-2013, 2013.

Juárez, R. I. N., M. G. Hodnett, R. Fu, M. L. Goulden, and C. von Randow, Control of Dry Season Evapotranspiration over the Amazonian Forest as Inferred from Observations at a Southern Amazon Forest Site, *J Climate*, *20*(12), 2827–2839, doi:10.1175/JCLI4184.1, 2007.

Jung, M., Reichstein, M., Schwalm, C.R., Huntingford, C., Sitch, S., Ahlström, A., Arneth, A., Camps-Valls, G., Ciais, P., Friedlingstein, P. and Gans, F., Compensatory water effects link yearly global land CO2 sink changes to temperature,, *541*(7638), 516–520, doi:10.1038/nature20780, 2017.

Kato, S., N. G. Loeb, F. G. Rose, D. R. Doelling, D. A. Rutan, T. E. Caldwell, L. Yu, and R. A. Weller, Surface Irradiances Consistent with CERES-Derived Top-of-Atmosphere Shortwave and Longwave Irradiances, *J Climate*, *26*(9), 2719–2740, doi:10.1175/JCLI-D-12-00436.1, 2013.

Keller, M., Alencar, A., Asner, G.P., Braswell, B., Bustamante, M., Davidson, E., Feldpausch, T., Fernandes, E., Goulden, M., Kabat, P. and Kruijt, B., Ecological Research in the Large-Scale Biosphere– Atmosphere Experiment in Amazonia: Early Results, *Ecol Appl*, *14*(sp4), 3–16, 2004.

Kennedy, D., Swenson, S., Oleson, K. W., Lawrence, D. M., Fisher, R., Lola da Costa, A. C., & Gentine, P. Implementing plant hydraulics in the Community Land Model, version 5. *Journal of Advances in Modeling Earth Systems*, *11*(2), 485-513, 2019.

Khairoutdinov, M., and D. Randall, High-resolution simulation of shallow-to-deep convection transition over land, *J Atmos Sci*, *63*(12), 3421–3436, 2006.

1319 Khanna, J., D. Medvigy, S. Fueglistaler, and R. Walko, Regional dry-season climate
1320 changes due to three decades of Amazonian deforestation, *Nature Climate Change*,
1321 *7*(3), 200–204, doi:10.1038/nclimate3226, 2017.

1322 Knox, R. G., M. Longo, A. L. S. Swann, K. Zhang, N. M. Levine, P. R. Moorcroft,
1323 and R. L. Bras, Hydrometeorological effects of historical land-conversion in an
1324 ecosystem-atmosphere model of Northern South America, *Hydrol Earth Syst Sc*,
1325 *19*(1), 241–273, doi:10.5194/hess-19-241-2015, 2015.

1326 Konings, A. G., and P. Gentine, Global variations in ecosystem-scale isohydricity,
1327 *Global Change Biol*, doi:10.1111/gcb.13389, 2016.

1328 Koren, I., Y. J. Kaufman, L. A. Remer, and J. V. Martins, Measurement of the effect
1329 of Amazon smoke on inhibition of cloud formation, *Science*, *303*(5662), 1342–1345,
1330 doi:10.1126/science.1089424, 2004.

1331 Koster, R.D., Dirmeyer, P.A., Guo, Z., Bonan, G., Chan, E., Cox, P., Gordon, C.T.,
1332 Kanae, S., Kowalczyk, E., Lawrence, D. and Liu, P., Regions of strong coupling
1333 between soil moisture and precipitation, *Science*, *305*(5687), 1138–1140, 2004.

1334 Koster, R.D., Dirmeyer, P.A., Guo, Z., Bonan, G., Chan, E., Cox, P., Gordon, C.T.,
1335 Kanae, S., Kowalczyk, E., Lawrence, D. and Liu, P., The Second Phase of the Global
1336 Land–Atmosphere Coupling Experiment: Soil Moisture Contributions to Subseasonal
1337 Forecast Skill, *J Hydrometeorol*, *12*(5), 805–822, doi:10.1175/2011JHM1365.1,
1338 2011.

1339 Köppen, W., *The thermal zones of the Earth according to the duration of hot,*
1340 *moderate and cold periods and of the impact of heat on the organic world.(translated*
1341 *and ...*, Meteorologische Zeitschrift, 1884.

1342 Krakauer, N. Y., M. J. Puma, B. I. Cook, P. Gentine, and L. Nazarenko, Ocean-
1343 atmosphere interactions modulate irrigation's climate impacts,, 1–16,
1344 doi:10.5194/esd-2016-23, 2016.

1345   Kuang, Z., Linear response functions of a cumulus ensemble to temperature and
1346   moisture perturbations and implications for the dynamics of convectively coupled
1347   waves, *J Atmos Sci,* 2010.

1348   Kuang, Z., A Moisture-Stratiform Instability for Convectively Coupled Waves,
1349   *Journal of Atmospheric Sciences*, *65*(3), 834–854, doi:10.1175/2007JAS2444.1,
1350   2008.

1351   Laan-Luijkx, I.T., Velde, I.R., Krol, M.C., Gatti, L.V., Domingues, L.G., Correia,
1352   C.S.C., Miller, J.B., Gloor, M., Leeuwen, T.T., Kaiser, J.W. and Wiedinmyer, C.,
1353   Response of the Amazon carbon balance to the 2010 drought derived with
1354   CarbonTracker South America, *Global Biogeochem Cy*, *29*(7), 1092–1108,
1355   doi:10.1002/2014GB005082, 2015.

1356   Laurent, H., L. Machado, and C. A. Morales, Characteristics of the Amazonian
1357   mesoscale convective systems observed from satellite and radar during the
1358   WETAMC/LBA experiment, *J of Climate,* 2002.

1359   Lawrence, D. M., K. W. Oleson, and M. G. Flanner, Parameterization improvements
1360   and functional and structural advances in Version 4 of the Community Land Model,
1361   *JAMES,* 2011

1362   Lawrence, D., and K. Vandecar, Effects of tropical deforestation on climate and
1363   agriculture, *Nature Climate Change*, *5*(1), 27–36, doi:10.1038/nclimate2430, 2015.

1364   Lawton, R. O., U. S. Nair, R. A. Pielke Sr, and R. M. Welch, Climatic Impact of
1365   Tropical Lowland Deforestation on Nearby Montane Cloud Forests, *Science*, *294*,
1366   584–587, 2001.

1367   Lebel, T., Cappelaere, B., Galle, S., Hanan, N., Kergoat, L., Levis, S., Vieux, B.,
1368   Descroix, L., Gosset, M., Mougin, E. and Peugeot, C., AMMA-CATCH studies in the
1369   Sahelian region of West-Africa: An overview, *Journal of Hydrology*, *375*(1-2), 3–13,
1370   doi:10.1016/j.jhydrol.2009.03.020, 2009.

1371   Lee, J. E., R. S. Oliveira, T. E. Dawson, and I. Fung, Root functioning modifies
1372   seasonal climate, *P Natl Acad Sci Usa*, *102*(49), 17576–17581, 2005.

1373   Lee, J.-E., J. A. Berry, C. van der Tol, X. Yang, L. Guanter, A. Damm, I. Baker, and
1374   C. Frankenberg, Simulations of chlorophyll fluorescence incorporated into the
1375   Community Land Model version 4, *Global Change Biol*, n/a–n/a,
1376   doi:10.1111/gcb.12948, 2015.

1377   Lemordant, L., Modification of land-atmosphere interactions by CO_2 effects:
1378   Implications for summer dryness and heat wave amplitude, *Geo Res Letters*, *43*(19),
1379   10–240–10–248, doi:10.1002/2016GL069896, 2016.

1380   Leuning, R., A critical appraisal of a combined stomatal-photosynthesis model for C3
1381   plants, *Plant Cell and Env*, 1995.

1382   Leuning, R., F. M. Kelliher, D. G. G. PURY, and E. D. Schulze, Leaf nitrogen,
1383   photosynthesis, conductance and transpiration: scaling from leaves to canopies, *Plant*
1384   *Cell Environ*, *18*(10), 1183–1200, doi:10.1111/j.1365-3040.1995.tb00628.x, 1995.

1385   Levy, M. C., A. Cohn, A. V. Lopes, and S. E. Thompson, Addressing rainfall data
1386   selection uncertainty using connections between rainfall and streamflow, *Sci. Rep.*,
1387   *7*(1), 1–12, doi:10.1038/s41598-017-00128-5, 2017.

1388   Li, W., R. Fu, and R. E. Dickinson, Rainfall and its seasonality over the Amazon in
1389   the 21st century as assessed by the coupled models for the IPCC AR4, *Journal of*
1390   *Geophysical Research*, 2006.

1391   Liebmann, B., and J. A. Marengo, Interannual variability of the rainy season and
1392   rainfall in the Brazilian Amazon basin, *J Climate*, *14*(22), 4308–4318, 2001.

1393   Lintner, B. R., and J. Chiang, Reorganization of tropical climate during El Nino: A
1394   weak temperature gradient approach, *J Climate*, *18*(24), 5312–5329, 2005.

1395   Lintner, B. R., and J. D. Neelin, A prototype for convective margin shifts, *Geophys*
1396   *Res Lett*, *34*(5), L05812, doi:10.1029/2006GL027305, 2007.

1397   Lintner, B. R., and J. D. Neelin, Soil Moisture Impacts on Convective Margins, *J*
1398   *Hydrometeorol*, *10*(4), 1026–1039, doi:10.1175/2009JHM1094.1, 2009.

1399   Lintner, B. R., P. Gentine, K. L. Findell, and G. D. Salvucci, The Budyko and
1400   complementary relationships in an idealized model of large-scale land–atmosphere
1401   coupling, *Hydrol Earth Syst Sc*, *19*(5), 2119–2131, doi:10.5194/hess-19-2119-2015,
1402   2015.

1403   Lintner, B. R., P. Gentine, K. L. Findell, F. D'Andrea, A. H. Sobel, and G. D.
1404   Salvucci, An idealized prototype for large-scale land-atmosphere coupling, *J Climate*,
1405   *26*(7), 2379–2389, doi:10.1175/JCLI-D-11-00561.1, 2013.

1406   Liu, L., L. Guan, and X. Liu, Directly estimating diurnal changes in GPP for C3 and
1407   C4 crops using far-red sun-induced chlorophyll fluorescence, *Agr Forest Meteorol*,
1408   *232*, 1–9, doi:10.1016/j.agrformet.2016.06.014, 2017.

1409   Lohou, F., F. Said, M. Lothon, P. Durand, and D. Serça, Impact of Boundary-Layer
1410   Processes on Near-Surface Turbulence Within the West African Monsoon, *Bound-*
1411   *Lay Meteorol*, *136*(1), 1–23, doi:10.1007/s10546-010-9493-0, 2010.

1412   Lopes, A. P., B. W. Nelson, J. Wu, P. M. L. de Alencastro Graça, J. V. Tavares, N.
1413   Prohaska, G. A. Martins, and S. R. Saleska, Leaf flush drives dry season green-up of
1414   the Central Amazon, *Remote Sensing of Environment*, *182*(C), 90–98,
1415   doi:10.1016/j.rse.2016.05.009, 2016.

1416   Machado, L.A., Silva Dias, M.A., Morales, C., Fisch, G., Vila, D., Albrecht, R.,
1417   Goodman, S.J., Calheiros, A.J., Biscaro, T., Kummerow, C. and Cohen, J.. The
1418   CHUVA project: How does convection vary across Brazil?. *Bulletin of the American*
1419   *Meteorological Society*, *95*(9), 1365-1380, 2014.

1420   Machado, L., and H. Laurent, Diurnal march of the convection observed during
1421   TRMM-WETAMC/LBA, *J Geo Res: Atmo*, 2002.

1422 Mahecha, M. D. et al., Global convergence in the temperature sensitivity of
1423 respiration at ecosystem level, *Science*, *329*(5993), 838–840,
1424 doi:10.1126/science.1189587, 2010.

1425 Malhi Y., A. D. Nobre, J. Grace, B. Kruijt, M. G. P. Pereira, A. Culf, S. Scott, Carbon
1426 dioxide transfer over a Central Amazonian rain forest. Journal of Geophysi- cal
1427 Research-Atmospheres 103, 31593-31612 (1998); published online EpubDec 27
1428 (10.1029/98jd02647).

1429 Marengo, J. A., J. Tomasella, L. M. Alves, W. R. Soares, and D. A. Rodriguez, The
1430 drought of 2010 in the context of historical droughts in the Amazon region, *Geophys*
1431 *Res Lett*, *38*(12), n/a–n/a, doi:10.1029/2011GL047436, 2011.

1432 Martin, S.T., Artaxo, P., Machado, L.A.T., Manzi, A.O., Souza, R.A.F., Schumacher,
1433 C., Wang, J., Andreae, M.O., Barbosa, H.M.J., Fan, J. and Fisch, G., Introduction:
1434 Observations and Modeling of the Green Ocean Amazon (GoAmazon2014/5), *Atmos.*
1435 *Chem. Phys*, *16*(8), 4785–4797, doi:10.5194/acp-16-4785-2016, 2016.

1436 Martin, S. T. et al., The Green Ocean Amazon Experiment (GoAmazon2014/5)
1437 Observes Pollution Affecting Gases, Aerosols, Clouds, and Rainfall over the Rain
1438 Forest, *Bull. Amer. Meteor. Soc.*, *98*(5), 981–997, doi:10.1175/BAMS-D-15-00221.1,
1439 2017.

1440 Martinez-Vilalta, J., and N. Garcia-Forner, Water potential regulation, stomatal
1441 behaviour and hydraulic transport under drought: deconstructing the iso/anisohydric
1442 concept, *Plant Cell Environ*, *40*(6), 962–976, doi:10.1111/pce.12846, 2016.

1443 Martinez-Vilalta, J., R. Poyatos, D. Aguadé, J. Retana, and M. Mencuccini, A new
1444 look at water transport regulation in plants, *New Phytologist*, doi:10.1111/nph.12912,
1445 2014.

1446 Maxwell, R. M., & Condon, L. E. (2016). Connections between groundwater flow
1447 and transpiration partitioning. *Science*, *353*(6297), 377-380.

1448   Medlyn, B. E., R. A. Duursma, D. Eamus, D. S. Ellsworth, I. C. Prentice, C. V. M.
1449   Barton, K. Y. Crous, P. De Angelis, M. Freeman, and L. Wingate, Reconciling the
1450   optimal and empirical approaches to modelling stomatal conductance, *Global Change*
1451   *Biol*, *17*(6), 2134–2144, doi:10.1111/j.1365-2486.2010.02375.x, 2011.

1452   Medlyn, B. E., R. A. Duursma, D. Eamus, D. S. Ellsworth, I. Colin Prentice, C. V. M.
1453   Barton, K. Y. Crous, P. Angelis, M. Freeman, and L. Wingate, Reconciling the
1454   optimal and empirical approaches to modelling stomatal conductance, *Global Change*
1455   *Biol*, *18*(11), 3476–3476, doi:10.1111/j.1365-2486.2012.02790.x, 2012.

1456   Medvigy, D., R. L. Walko, and R. Avissar, Effects of Deforestation on
1457   Spatiotemporal Distributions of Precipitation in South America, *J Climate*, *24*, 2147–
1458   2163, 2011.

1459   Miralles, D. G., J. H. Gash, T. R. H. Holmes, R. A. M. de Jeu, and A. J. Dolman,
1460   Global canopy interception from satellite observations, *J Geophys Res*, *115*(D16),
1461   237, doi:10.1029/2009JD013530, 2010.

1462   Morton, D. C., and B. D. Cook, Amazon forest structure generates diurnal and
1463   seasonal variability in light utilization, *Biogeosciences*, *13*(7), 2195–2206,
1464   doi:10.5194/bg-13-2195-2016, 2016.

1465   Morton, D. C., J. Nagol, C. C. Carabajal, J. Rosette, M. Palace, B. D. Cook, E. F.
1466   Vermote, D. J. Harding, and P. R. J. North, Amazon forests maintain consistent
1467   canopy structure and greenness during the dry season, *Nature*, *506*(7487), 221–224,
1468   doi:10.1038/nature13006, 2014.

1469   Mueller, B., Seneviratne, S.I., Jimenez, C., Corti, T., Hirschi, M., Balsamo, G., Ciais,
1470   P., Dirmeyer, P., Fisher, J.B., Guo, Z. and Jung, M., Evaluation of global
1471   observations-based evapotranspiration datasets and IPCC AR4 simulations, *Geophys*
1472   *Res Lett*, *38*, –, doi:10.1029/2010GL046230, 2011.

1473   Munger, J. W., J. B. McManus, D. D. Nelson, M. S. Zahniser, E. A. Davidson, S. C.
1474   Wofsy, R. Wehr, and S. R. Saleska, Seasonality of temperate forest photosynthesis

1475 and daytime respiration, *Nature*, *534*(7609), 680–683, doi:10.1038/nature17966,
1476 2016.

1477 Nakicenovic, N., IPCC Special Report on Emissions Scenarios, 2000

1478 Naudts, K., Ryder, J., McGrath, M.J., Otto, J., Chen, Y., Valade, A., Bellasen, V.,
1479 Berhongaray, G., Bönisch, G., Campioli, M. and Ghattas, J., A vertically discretised
1480 canopy description for ORCHIDEE (SVN r2290) and the modifications to the energy,
1481 water and carbon fluxes, *Geosci. Model Dev. Discuss.*, *7*(6), 8565–8647,
1482 doi:10.5194/gmdd-7-8565-2014, 2014.

1483 Ngo-Duc, T., K. Laval, G. Ramillien, J. Polcher, and A. Cazenave, Validation of the
1484 land water storage simulated by Organising Carbon and Hydrology in Dynamic
1485 Ecosystems (ORCHIDEE) with Gravity Recovery and Climate Experiment (GRACE)
1486 data, *Water resources Research*, *43*(4), –, doi:10.1029/2006WR004941, 2007.

1487 Nicholson, S., Land surface processes and Sahel climate, *Rev Geophys*, *38*(1), 117–
1488 139, 2000.

1489 Nitta, T., Convective Activities in the Tropical Western Pacific and Their Impact on
1490 the Northern Hemisphere Summer Circulation, *Journal of the Meteorological Society*
1491 *of Japan. Ser. II*, *65*(3), 373–390, doi:10.2151/jmsj1965.65.3_373, 1987.

1492 Naudts, K., Ryder, J., McGrath, M.J., Otto, J., Chen, Y., Valade, A., Bellasen, V.,
1493 Berhongaray, G., Bönisch, G., Campioli, M. and Ghattas, J., The community Noah
1494 land surface model with multiparameterization options (Noah-MP): 1. Model
1495 description and evaluation with local-scale measurements, *J Geophys Res-Atmos*,
1496 *116*, –, doi:10.1029/2010JD015139, 2011.

1497 Noilhan, J., and S. Planton, A simple parameterization of land surface processes for
1498 meteorological models, *Mon Wea Rev*, 1989.

1499 Oleson, K.W., Niu, G.Y., Yang, Z.L., Lawrence, D.M., Thornton, P.E., Lawrence,
1500 P.J., Stöckli, R., Dickinson, R.E., Bonan, G.B., Levis, S. and Dai, A., Improvements
1501 to the Community Land Model and their impact on the hydrological cycle, *J Geophys*

Res-Biogeo, 113, –, doi:10.1029/2007JG000563, 2008.Oliveira, R. S., T. E. Dawson, S. S. O. Burgess, and D. C. Nepstad, Hydraulic redistribution in three Amazonian trees, *Oecologia*, *145*(3), 354–363, doi:10.1007/s00442-005-0108-2, 2005.

Liu, H., Gleason, S. M., Hao, G., Hua, L., He, P., Goldstein, G., & Ye, Q. (2019). Hydraulic traits are coordinated with maximum plant height at the global scale. *Science Advances*, *5*(2), eaav1332. https://doi.org/10.1126/sciadv.aav1332

Oliveira, R.S., Dawson, T.E., Burgess, S.S.O. (2005) *Oecologia* 145: 354. https://doi.org/10.1007/s00442-005-0108-2

Ometto, J. P. H. B., Ehleringer, J. R., Domingues, T. F., Berry, J. A., Ishida, F. Y., Mazzi, E., et al. (2006). The stable carbon and nitrogen isotopic composition of vegetation in tropical forests of the Amazon Basin, Brazil. *Biogeochemistry*, *79*(1–2), 251–274. https://doi.org/10.1007/s10533-006-9008-8

Ouwersloot, H. G., J. V.-G. de Arellano, B. J. H. van Stratum, M. C. Krol, and J. Lelieveld, Quantifying the transport of sub-cloud layer reactants by shallow cumulus clouds over the Amazon, *J Geophys Res-Atmos*, n/a–n/a, doi:10.1002/2013JD020431, 2013.

Pagán, B. R., Maes, W. H., Gentine, P., Martens, B., & Miralles, D. G. (2019). Exploring the Potential of Satellite Solar-Induced Fluorescence to Constrain Global Transpiration Estimates. *Remote Sensing*, *11*(4), 413. https://doi.org/10.3390/rs11040413

Park, S., and C. S. Bretherton, The University of Washington Shallow Convection and Moist Turbulence Schemes and Their Impact on Climate Simulations with the Community Atmosphere Model, *J Climate*, *22*(12), 3449–3469, doi:10.1175/2008JCLI2557.1, 2009.

Park, S.-B., S. Boeing, and P. Gentine, Role of shear on shallow convection (in press), *J Atmos Science*, 2018.

1528   Perduzo-Bagazgoitia X., Ouwersloot H.G., Sikma M., van Heerwaarden C.C., Jacobs

1529   C. M. and Vilà-Guerau de Arellano J (2017) Direct and diffuse radiation in the

1530   shallow cumulus-vegetation system: enhanced and decreased evapotranspiration

1531   regimes. J. Hydrometeorology 18, 1731-1748.

1532

1533   Peterhansel, C., and V. G. Maurino, Photorespiration Redesigned, *Plant Physiol*,

1534   *155*(1), 49–55, doi:10.1104/pp.110.165019, 2011.

1535   Phillips, N. G., R. Oren, J. Licata, and S. Linder, Time series diagnosis of tree

1536   hydraulic characteristics, *Tree Physiol*, 879–890, 2004.

1537   Phillips, N. G., T. N. Buckley, and D. T. Tissue, Capacity of Old Trees to Respond to

1538   Environmental Change, *Journal of Integrative Plant Biology*, *50*(11), 1355–1364,

1539   doi:10.1111/j.1744-7909.2008.00746.x, 2008.

1540   Phillips, N., A. Nagchaudhuri, R. Oren, and G. Katul, Time constant for water

1541   transport in loblolly pine trees estimated from time series of evaporative demand and

1542   stem sapflow, *Trees*, *11*(7), 412–419, 1997.

1543   Pielke Sr, R.A., Pitman, A., Niyogi, D., Mahmood, R., McAlpine, C., Hossain, F.,

1544   Goldewijk, K.K., Nair, U., Betts, R., Fall, S. and Reichstein, M., Land use/land cover

1545   changes and climate: modeling analysis and observational evidence, *Wires Clim*

1546   *Change*, *2*(6), 828–850, doi:10.1002/wcc.144, 2011.

1547   Pielke, R. A., Sr, R. Mahmood, and C. McAlpine, Land's complex role in climate

1548   change, *Physics Today*, *69*(11), 40–46, doi:10.1063/PT.3.3364, 2016.

1549   Pielke, R., and R. Avissar, Influence of landscape structure on local and regional

1550   climate, *Landscape Ecology*, *4*(2/3), 133–155, 1990.

1551   Pielke, R., G. DALU, J. SNOOK, T. LEE, and T. KITTEL, Nonlinear Influence of

1552   Mesoscale Land-Use on Weather and Climate, *J Climate*, *4*(11), 1053–1069, 1991.

1553   Pons, T. L., and R. Welschen, Midday depression of net photosynthesis in the tropical
1554   rainforest tree Eperua grandiflora: contributions of stomatal and internal
1555   conductances, respiration and Rubisco functioning, *Tree Physiol*, *23*(14), 937–947,
1556   2003.

1557   Poulter, B., Frank, D., Ciais, P., Myneni, R.B., Andela, N., Bi, J., Broquet, G.,
1558   Canadell, J.G., Chevallier, F., Liu, Y.Y. and Running, S.W., Contribution of semi-
1559   arid ecosystems to interannual variability of the global carbon cycle, *Nature*,
1560   *509*(7502), 600–603, doi:10.1038/nature13376, 2014.

1561   Powell, T.L., Galbraith, D.R., Christoffersen, B.O., Harper, A., Imbuzeiro, H.M.,
1562   Rowland, L., Almeida, S., Brando, P.M., da Costa, A.C.L., Costa, M.H. and Levine,
1563   N.M., Confronting model predictions of carbon fluxes with measurements of Amazon
1564   forests subjected to experimental drought, *New Phytologist*, *200*(2), 350–365,
1565   doi:10.1111/nph.12390, 2013.

1566   Pradipta, P., A. Giannini, P. Gentine, and U. Lall, Resolving Contrasting Regional
1567   Rainfall Responses to El Niño over Tropical Africa, *J Climate*, *29*(4), 1461–1476,
1568   doi:10.1175/JCLI-D-15-0071.1, 2016.

1569   Prieto, I., and R. J. Ryel, Internal hydraulic redistribution prevents the loss of root
1570   conductivity during drought, *Tree Physiol*, *34*(1), 39–48,
1571   doi:10.1093/treephys/tpt115, 2014.

1572   Ray, D. K., U. S. Nair, R. O. Lawton, R. M. Welch, and R. A. Pielke Sr. Impact of
1573   land use on Costa Rican tropical montane cloud forests: Sensitivity of orographic
1574   cloud formation to deforestation in the plains, *J Geophys Res*, *111*(D2), D02108,
1575   doi:10.1029/2005JD006096, 2006.

1576   Raymond, D. J., and X. Zeng, Modelling tropical atmospheric convection in the
1577   context of the weak temperature gradient approximation, *Q J Roy Meteor Soc*,
1578   *131*(608), 1301–1320, doi:10.1256/qj.03.97, 2005.

1579   Redelsperger, J.-L., C. D. Thorncroft, A. Diedhiou, T. Lebel, D. J. Parker, and J.
1580   Polcher African monsoon multidisciplinary analysis - An international research
1581   project and field campaign, *Bull. Amer. Meteor. Soc.*, *87*(12), 1739–+,
1582   doi:10.1175/BAMS-87-12-1739, 2006.

1583   Restrepo-Coupe, N., da Rocha, H.R., Hutyra, L.R., da Araujo, A.C., Borma, L.S.,
1584   Christoffersen, B., Cabral, O.M., de Camargo, P.B., Cardoso, F.L., da Costa, A.C.L.
1585   and Fitzjarrald, D.R., What drives the seasonality of photosynthesis across the
1586   Amazon basin? A cross-site analysis of eddy flux tower measurements from the
1587   Brasil flux network, *Agr Forest Meteorol*, *182-183*, 128–144,
1588   doi:10.1016/j.agrformet.2013.04.031, 2013.

1589   Rickenbach, T. M., Ferreira, R. N., Halverson, J. B., Herdies, D. L., & Dias, M. A. S.
1590   (2002). Modulation of convection in the southwestern Amazon basin by extratropical
1591   stationary fronts. *Journal of Geophysical Research: Atmospheres*, *107*(D20), LBA-7.

1592   Rieck, M., C. Hohenegger, and C. C. van Heerwaarden, The influence of land surface
1593   heterogeneities on cloud size development, *Mon Wea Rev*, 140611124045000,
1594   doi:10.1175/MWR-D-13-00354.1, 2014.

1595   Rieck, M., C. Hohenegger, and P. Gentine, The effect of moist convection on
1596   thermally induced mesoscale circulations, *Q J Roy Meteor Soc*, *141*(691), 2418–2428,
1597   doi:10.1002/qj.2532, 2015.

1598   Rio, C., F. Hourdin, J. Y. Grandpeix, and J. P. Lafore, Shifting the diurnal cycle of
1599   parameterized deep convection over land, *Geophys Res Lett*, *36*, –,
1600   doi:10.1029/2008GL036779, 2009.

1601   Rochetin, N., F. Couvreux, J.-Y. Grandpeix, and C. Rio, Deep Convection Triggering
1602   by Boundary Layer Thermals. Part I: LES Analysis and Stochastic Triggering
1603   Formulation, *J Atmos Sci*, *71*(2), 496–514, doi:10.1175/JAS-D-12-0336.1, 2014.

1604   Rochetin, N., J.-Y. Grandpeix, C. Rio, and F. Couvreux, Deep Convection Triggering
1605   by Boundary Layer Thermals. Part II: Stochastic Triggering Parameterization for the
1606   LMDZ GCM, *J Atmos Sci*, *71*(2), 515–538, doi:10.1175/JAS-D-12-0337.1, 2014.

1607   Romps, D. M., Numerical tests of the weak pressure gradient approximation, *J Atmos
1608   Sci*, *69*(9), 2846–2856, doi:10.1175/JAS-D-11-0337.1, 2012.

1609   Romps, D. M., Weak Pressure Gradient Approximation and Its Analytical Solutions,
1610   *J Atmos Sci*, *69*(9), 2835–2845, doi:10.1175/JAS-D-11-0336.1, 2012.

1611   Roy, S., C. Weaver, D. Nolan, and R. Avissar, A preferred scale for landscape forced
1612   mesoscale circulations? *J Geophys Res-Atmos*, *108*(D22), 8854,
1613   doi:10.1029/2002JD003097, 2003.

1614   Saatchi, S., S. Asefi-Najafabady, Y. Malhi, L. E. O. C. Aragao, L. O. Anderson, R. B.
1615   Myneni, and R. Nemani, Persistent effects of a severe drought on Amazonian forest
1616   canopy, *PNAS*, *110*(2), 565–570, doi:10.1073/pnas.1204651110, 2013.

1617   Saleska, S. R., J. Wu, K. Guan, A. C. Araujo, and A. Huete, Dry-season greening of
1618   Amazon forests, *Nature*, doi:10.1038/nature16457, 2016.

1619   Schaefli, B., R. J. van der Ent, R. Woods, and H. H. G. Savenije, An analytical model
1620   for soil-atmosphere feedback, *Hydrol Earth Syst Sc*, *16*(7), 1863–1878,
1621   doi:10.5194/hess-16-1863-2012, 2012.

1622   Schiro, K. A., J. D. Neelin, D. K. Adams, and B. R. Lintner, Deep Convection and
1623   Column Water Vapor over Tropical Land versus Tropical Ocean: A Comparison
1624   between the Amazon and the Tropical Western Pacific, *Journal of Atmospheric
1625   Sciences*, *73*(10), 4043–4063, doi:10.1175/JAS-D-16-0119.1, 2016.

1626   Scholz, F., N. Phillips, and S. Bucci, Hydraulic capacitance: biophysics and
1627   functional significance of internal water sources in relation to tree size, *Size- and Age-
1628   Related Changes in Tree Structure*, 341–361, 2011.

1629   Scott, R., D. Entekhabi, R. D. Koster, and M. Suarez, Timescales of land surface
1630   evapotranspiration response, *J Climate*, *10*(4), 559–566, 1997.

1631   Sellers, P. J., C. J. Tucker, G. J. Collatz, S. O. Los, C. O. Justice, D. A. Dazlich, and
1632   D. A. Randall, A Revised Land Surface Parameterization (SiB2) for Atmospheric
1633   GCMS. Part II: The Generation of Global Fields of Terrestrial Biophysical
1634   Parameters from Satellite Data, *J Climate*, *9*(4), 706–737, doi:10.1175/1520-
1635   0442(1996)009<0706:ARLSPF>2.0.CO;2, 1996.

1636   Sellers, P., D. A. Randall, G. Collatz, J. Berry, C. Field, D. Dazlich, C. Zhang, G.
1637   Collelo, and L. Bounoua, A Revised Land Surface Parameterization (SiB2) for
1638   Atmospheric GCMS. Part I: Model Formulation, *J Climate*, *9*(4), 676–705, 1996.

1639   Seneviratne, S., Impact of soil moisture-climate feedbacks on CMIP5 projections:
1640   First results from the GLACE-CMIP5 experiment, *Geophys Res Lett*, *40*(19), 5212–
1641   5217, doi:10.1002/grl.50956, 2013.

1642   Sentić, S., and S. L. Sessions, Idealized modeling of convective organization with
1643   Changing Sea surface temperatures using multiple equilibria in weak temperature
1644   gradient simulations, *J. Adv. Model. Earth Syst.*, 1–65, doi:10.1002/2016MS000873,
1645   2017.

1646   Stohl, A., & James, P. (2005). A Lagrangian analysis of the atmospheric branch of the
1647   global water cycle. Part II: Moisture transports between earth's ocean basins and river
1648   catchments. *Journal of Hydrometeorology*, *6*(6), 961-984.

1649   Sobel, A. H., and C. S. Bretherton, Large-scale waves interacting with deep
1650   convection in idealized mesoscale model simulations, *Tellus Series A-Dynamic*
1651   *Meteorology And Oceanography*, *55*(1), 45–60, doi:10.1034/j.1600-
1652   0870.2003.201421.x, 2003.

1653   Sobel, A. H., G. Bellon, and J. Bacmeister, Multiple equilibria in a single-column
1654   model of the tropical atmosphere, *Geophys Res Lett*, *34*(22), L22804,
1655   doi:10.1029/2007GL031320, 2007.

1656   Sobel, A. H., J. Nilsson, and L. Polvani, The weak temperature gradient
1657   approximation and balanced tropical moisture waves, *J Atmos Sci*, *58*(23), 3650–
1658   3665, 2001.

1659   Spracklen, D. V., S. R. Arnold, and C. M. Taylor, Observations of increased tropical
1660   rainfall preceded by air passage over forests, *Nature*, *489*(7415), 282–285,
1661   doi:10.1038/nature11390, 2012.

1662   Stevens, B., and S. Bony, What Are Climate Models Missing? *Science*, *340*(6136),
1663   1053–1054, doi:10.1126/science.1237554, 2013.

1664   Stoeckli, R., D. M. Lawrence, G. Y. Niu, K. W. Oleson, P. E. Thornton, Z. L. Yang,
1665   G. B. Bonan, A. S. Denning, and S. W. Running, Use of FLUXNET in the
1666   Community Land Model development, *J Geophys Res*, *113*(G1), G01025,
1667   doi:10.1029/2007JG000562, 2008.

1668   Sutanto, S. J., J. Wenninger, A. M. J. Coenders-Gerrits, and S. Uhlenbrook,
1669   Partitioning of evaporation into transpiration, soil evaporation and interception: a
1670   comparison between isotope measurements and a HYDRUS-1D model, *Hydrol Earth
1671   Syst Sc*, *16*(8), 2605–2616, doi:10.5194/hess-16-2605-2012, 2012.

1672   Swann, A. L. S., M. Longo, R. G. Knox, E. Lee, and P. R. Moorcroft, Future
1673   deforestation in the Amazon and consequences for South American climate, *Agr
1674   Forest Meteorol*, *214-215*, 12–24, doi:10.1016/j.agrformet.2015.07.006, 2015.

1675   Tang, S., Xie, S., Zhang, Y., Zhang, M., Schumacher, C., Upton, H., Jensen, M.P.,
1676   Johnson, K.L., Wang, M., Ahlgrimm, M. and Feng, Z., Large-scale vertical velocity,
1677   diabatic heating and drying profiles associated with seasonal and diurnal variations of
1678   convective systems observed in the GoAmazon2014/5 experiment, *Atmos. Chem.
1679   Phys*, *16*(22), 14249–14264, doi:10.5194/acp-16-14249-2016, 2016.

1680   Tawfik, A. B., & Dirmeyer, P. A. (2014). A process-based framework for quantifying
1681   the atmospheric preconditioning of surface-triggered convection. *Geophysical
1682   Research Letters*, *41*(1), 173-178.

1683   Tawfik, A. B., Dirmeyer, P. A., & Santanello Jr, J. A. (2015). The heated
1684   condensation framework. Part I: Description and Southern Great Plains case study.
1685   *Journal of Hydrometeorology*, *16*(5), 1929-1945.

1686   Tawfik, A. B., Dirmeyer, P. A., & Santanello Jr, J. A. (2015). The heated
1687   condensation framework. Part II: Climatological behavior of convective initiation and
1688   land–atmosphere coupling over the conterminous United States. *Journal of*
1689   *Hydrometeorology*, *16*(5), 1946-1961.

1690   Taylor, C. M., C. E. Birch, D. J. Parker, N. Dixon, F. Guichard, G. Nikulin, and G.
1691   M. S. Lister, New perspectives on land-atmosphere feedbacks from the African
1692   Monsoon Multidisciplinary Analysis, *Atmos Sci Lett*, *12*(1), 38–44,
1693   doi:10.1002/asl.336, 2011.

1694   Taylor, C. M., C. E. Birch, D. J. Parker, N. Dixon, F. Guichard, G. Nikulin, and G.
1695   M. S. Lister, Modelling soil moisture - precipitation feedbacks in the Sahel:
1696   importance of spatial scale versus convective parameterization, *Geophys Res Lett*,
1697   *40*(23), 6213–6218, doi:10.1002/2013GL058511, 2013.

1698   Taylor, C. M., D. J. Parker, and P. P. Harris, An observational case study of
1699   mesoscale atmospheric circulations induced by soil moisture, *Geophys Res Lett*,
1700   *34*(15), L15801, doi:10.1029/2007GL030572, 2007.

1701   Taylor, C. M., P. P. Harris, and D. J. Parker, Impact of soil moisture on the
1702   development of a Sahelian mesoscale convective system: a case-study from the
1703   AMMA Special Observing Period, *Q J Roy Meteor Soc*, *136*(S1), 456–470,
1704   doi:10.1002/qj.465, 2009.

1705   Thiery, W., E. L. Davin, D. M. Lawrence, A. L. Hirsch, M. Hauser, and S. I.
1706   Seneviratne, Present-day irrigation mitigates heat extremes, *J Geophys Res-Atmos*,
1707   *122*(3), 1403–1422, doi:10.1002/2016JD025740, 2017.

1708   Thornley, J. H. M., Plant growth and respiration re-visited: maintenance respiration
1709   defined - it is an emergent property of, not a separate process within, the system - and

why the respiration : photosynthesis ratio is conservative, *Annals of Botany*, *108*(7), 1365–1380, doi:10.1093/aob/mcr238, 2011.

Thum, T., Zaehle, S., Köhler, P., Aalto, T., Aurela, M., Guanter, L., Kolari, P., Laurila, T., Lohila, A., Magnani, F. and Tol, C.V.D., Modelling sun-induced fluorescence and photosynthesis with a land surface model at local and regional scales in northern Europe, *Biogeosciences*, *14*(7), 1969–1987, doi:10.5194/bg-14-1969-2017, 2017.

Torri, G., Z. Kuang, and Y. Tian, Mechanisms for convection triggering by cold pools, *Geophys Res Lett*, *42*(6), 1943–1950, doi:10.1002/2015GL063227, 2015.

Trenberth, Kevin E. (1999). Atmospheric Moisture Recycling: Role of Advection and Local Evaporation. *Journal of Climate*. 12 (5): 1368–1381. doi:10.1175/1520-0442(1999)012<1368:amrroa>2.0.co;2

van der Ent, R. J., and O. A. Tuinenburg, The residence time of water in the atmosphere revisited, *Hydrol Earth Syst Sc*, *21*(2), 779–790, doi:10.5194/hess-21-779-2017, 2017.

van der Ent, R. J., H. H. G. Savenije, B. Schaefli, and S. C. Steele-Dunne, Origin and fate of atmospheric moisture over continents, *Water resources Research*, *46*(9), doi:10.1029/2010WR009127, 2010.

van Dijk, A.I., Gash, J.H., van Gorsel, E., Blanken, P.D., Cescatti, A., Emmel, C., Gielen, B., Harman, I.N., Kiely, G., Merbold, L. and Montagnani, L., Rainfall interception and the coupled surface water and energy balance, *Agr Forest Meteorol*, *214-215*, 402–415, doi:10.1016/j.agrformet.2015.09.006, 2015.

Vila-Guerau de Arellano, J., E. G. Patton, T. Karl, K. van den Dries, M. C. Barth, and J. J. Orlando, The role of boundary layer dynamics on the diurnal evolution of isoprene and the hydroxyl radical over tropical forests, *J Geophys Res-Atmos*, *116*(D7), 8032, doi:10.1029/2010JD014857, 2011.

1736 Vogel, M. M., R. Orth, F. Cheruy, S. Hagemann, R. Lorenz, B. J. J. M. van den Hurk,
1737 and S. I. Seneviratne, Regional amplification of projected changes in extreme
1738 temperatures strongly controlled by soil moisture-temperature feedbacks, *Geophys*
1739 *Res Lett*, *44*(3), 1511–1519, doi:10.1002/2016GL071235, 2017.

1740 Vourlitis, G., et al., 2001: Seasonal variations in the net ecosystem CO exchange of a
1741 mature Amazonian transitional tropical forest (cerradão). *Functional Ecology* 2001
1742 15, 388–395

1743 Vourlitis, G., et al., 2002: Seasonal variations in the evapotranspiration of a
1744 transitional tropical forest of Mato Grosso, Brazil. *Water resources research*, 38, 6,
1745 1094, 10.1029/2000WR000122

1746 Vourlitis et al., 2008: Energy balance and canopy conductance of a tropical semi-
1747 deciduous forest of the southern Amazon Basin. *Water resources research,* 44,
1748 W03412, doi:10.1029/2006WR005526

1749 Vourlitis, G., et al., 2004: EFFECTS OF METEOROLOGICAL VARIATIONS ON
1750 THE CO_2 EXCHANGE OF A BRAZILIAN TRANSITIONAL TROPICAL
1751 FOREST. *Ecological Applications,* 14(4) 2004, S89–S100
1752

1753 Vourlitis et al., 2005: The Sensitivity of Diel CO_2 and H_2O Vapor Exchange of a
1754 Tropical Transitional Forest to Seasonal Variation in Meteorology and Water
1755 Availability. *Earth Interactions* 9 27

1756 Wang, J., F. J. F. Chagnon, E. R. Williams, A. K. Betts, N. O. Renno, L. A. T.
1757 Machado, G. Bisht, R. Knox, and R. L. Bras, Impact of deforestation in the Amazon
1758 basin on cloud climatology, *PNAS*, *106*(10), 3670–3674,
1759 doi:10.1073/pnas.0810156106, 2009.

1760 Wang, J., R. L. Bras, and E. Eltahir, The impact of observed deforestation on the
1761 mesoscale distribution of rainfall and clouds in Amazonia, *J Hydrometeorol*, *1*(3),
1762 267–286, 2000.

1763 Wang, S., A. H. Sobel, and Z. Kuang, Cloud-resolving simulation of TOGA-COARE
1764 using parameterized large-scale dynamics, *J Geophys Res-Atmos*, *118*(12), 6290–
1765 6301, doi:10.1002/jgrd.50510, 2013.

1766 Wang, Y. P., and R. Leuning, A two-leaf model for canopy conductance,
1767 photosynthesis and partitioning of available energy I:, *Agr Forest Meteorol*, *91*(1-2),
1768 89–111, doi:10.1016/S0168-1923(98)00061-6, 1998.

1769 Washington, R., R. James, H. Pearce, W. M. Pokam, and W. Moufouma-Okia, Congo
1770 Basin rainfall climatology: can we believe the climate models? *Philos T R Soc B*,
1771 *368*(1625), 20120296–20120296, doi:10.1098/rstb.2012.0296, 2013.

1772 Wehr, R., R. Commane, J. W. Munger, J. B. McManus, D. D. Nelson, M. S. Zahniser,
1773 S. R. Saleska, and S. C. Wofsy, Dynamics of canopy stomatal conductance,
1774 transpiration, and evaporation in a temperate deciduous forest, validated by carbonyl
1775 sulfide uptake,, 1–17, doi:10.5194/bg-2016-365, 2016.

1776 Werth, D., and R. Avissar, The local and global effects of Amazon deforestation, *J*
1777 *Geophys Res-Atmos*, *107*(D20), 8087, doi:10.1029/2001JD000717, 2002.

1778 Williams M., Y. Malhi, A. D. Nobre, E. B. Rastetter, J. Grace, M. G. P. Pereira, Seasonal
1779 variation in net carbon exchange and evapotranspiration in a Brazilian rain forest: a
1780 modelling analysis. Plant Cell and Environment 21, 953-968 (1998); published online
1781 EpubOct (10.1046/j.1365-3040.1998.00339.x).

1782

1783 Wills, R. C., M. P. Byrne, and T. Schneider, Thermodynamic and dynamic controls
1784 on changes in the zonally anomalous hydrological cycle, *Geo Res Letters*, *43*(9),
1785 4640–4649, doi:10.1002/2016GL068418, 2016.

1786 Wright, J. S., R. Fu, J. R. Worden, S. Chakraborty, N. E. Clinton, C. Risi, Y. Sun, and
1787 L. Yin, Rainforest-initiated wet season onset over the southern Amazon, *PNAS*,
1788 *114*(32), 8481–8486, doi:10.1073/pnas.1621516114, 2017.

1789 Wu, C.-M., B. Stevens, and A. Arakawa, What Controls the Transition from Shallow
1790 to Deep Convection? *J Atmos Sci*, *66*(6), 1793–1806, doi:10.1175/2008JAS2945.1,
1791 2009.

1792   Xu, X., D. Medvigy, J. S. Powers, J. M. Becknell, and K. Guan, Diversity in plant
1793   hydraulic traits explains seasonal and inter-annual variations of vegetation dynamics
1794   in seasonally dry tropical forests, *New Phytologist*, 1–16, doi:10.1111/nph.14009,
1795   2016.

1796   Yano, J. I., and R. S. Plant, Convective quasi-equilibrium, *Rev Geophys*, *50*(4),
1797   RG4004, doi:10.1029/2011RG000378, 2012.

1798   Yin, L., R. Fu, E. Shevliakova, and R. E. Dickinson, How well can CMIP5 simulate
1799   precipitation and its controlling processes over tropical South America? *Climate*
1800   *dynamics*, *41*(11-12), 3127–3143, doi:10.1007/s00382-012-1582-y, 2013.

1801   Yu, H., L. A. Remer, M. Chin, H. Bian, R. G. Kleidman, and T. Diehl, A satellite-
1802   based assessment of transpacific transport of pollution aerosol, *J Geophys Res-Atmos*,
1803   *113*(D14), doi:10.1029/2007JD009349, 2008.

1804   Zahn, E., N. L. Dias, A. Araújo, L. D. A. Sá, M. Sörgel, I. Trebs, S. Wolff, and A.
1805   Manzi, Scalar turbulent behavior in the roughness sublayer of an Amazonian forest,
1806   *Atmos. Chem. Phys*, *16*(17), 11349–11366, doi:10.5194/acp-16-11349-2016, 2016.

1807   Zeng, N., and J. D. Neelin, A land-atmosphere interaction theory for the tropical
1808   deforestation problem, *J Climate*, *12*(2-3), 857–872, 1999.

1809   Zeng, N., J. Neelin, K. Lau, and C. Tucker, Enhancement of Interdecadal Climate
1810   Variability in the Sahel by Vegetation Interaction, *Science*, *286*(5444), 1537–1540,
1811   1999.

1812   Zeppel, M. J. B., J. D. Lewis, N. G. Phillips, and D. T. Tissue, Consequences of
1813   nocturnal water loss: a synthesis of regulating factors and implications for
1814   capacitance, embolism and use in models, *Tree Physiol*, *34*(10), 1047–1055,
1815   doi:10.1093/treephys/tpu089, 2014.

1816   Zhang, K., de Almeida Castanho, A.D., Galbraith, D.R., Moghim, S., Levine, N.M.,
1817   Bras, R.L., Coe, M.T., Costa, M.H., Malhi, Y., Longo, M. and Knox, R.G., The fate
1818   of Amazonian ecosystems over the coming century arising from changes in climate,

1819   atmospheric CO 2,and land use, *Global Change Biol*, *21*(7), 2569–2587,
1820   doi:10.1111/gcb.12903, 2015.

1821   Zhang, Y. J., F. C. Meinzer, and J. Qi, Midday stomatal conductance is more related
1822   to stem rather than leaf water status in subtropical deciduous and evergreen broadleaf
1823   trees, *Plant Cell and Env*, *36*(1), 149–158, doi:10.1111/j.1365-3040.2012.02563.x,
1824   2013.

1825   Zhang, Y., R. Fu, H. Yu, R. E. Dickinson, R. N. Juarez, M. Chin, and H. Wang, A
1826   regional climate model study of how biomass burning aerosol impacts land-
1827   atmosphere interactions over the Amazon, *Journal of Geophysical Research:*
1828   *Atmospheres (1984–2012)*, *113*(D14), 1042, doi:10.1029/2007JD009449, 2008.

1829   Zhang, Y., R. Fu, H. Yu, Y. Qian, R. Dickinson, M. A. F. Silva Dias, P. L. da Silva
1830   Dias, and K. Fernandes, Impact of biomass burning aerosol on the monsoon
1831   circulation transition over Amazonia, *Geophys Res Lett*, *36*(10), 1509,
1832   doi:10.1029/2009GL037180, 2009.

1833   Zhuang, Y., R. Fu, and J. A. Marengo, Seasonal variation of shallow-to-deep
1834   convection transition and its link to the environmental conditions over the Central
1835   Amazon, *J Geo Res: Atmo*, doi:10.1002/(ISSN)2169-8996, 2017.

1836

1837

1838

1839   Table 1. The surface friction velocity, subcloud layer height (where the minimum of

1840   virtual potential temperature flux occurs), ratio of subcloud layer height and Obukhov

1841   length, ratio of surface friction velocity and Deardorff convective velocity scale, and the

1842   total number of identified clouds for 12 time instants in each case.

Case	S3	S2	S1	CTL	R1	R2	R3
$u_*\ u_*$ [m s^{-1}]	0.07	0.14	0.21	0.28	0.35	0.42	0.56
z_i [m]	590	590	590	590	590	610	630
$z_i\ /\ L$	392.1	49.0	14.5	6.1	3.1	1.9	0.8
$u_*/\ w_*$ $u_*/\ w_*$	0.10	0.20	0.30	0.40	0.50	0.60	0.79
N_{cloud}	2248	2229	2283	2302	2250	2703	2776

1843

1844

1845

1846

1847

1848

1849

1850

1851

1852

1853

1854

1855

1856

1889 Figure 12: Land-atmosphere feedback strength (change in the variance due to the
1890 feedback) between Precipitation and ET (top) and Photosynthetically Active Radiation
1891 (PAR) (bottom) based on recent metric developed by Green et al. [2017] using a
1892 multivariate Granger causality approach.

1893 Figure 13: (a) Schematic of the key elements of the convective margins framework as
1894 applied along an inflow path across northeastern South America. The solid blue and
1895 black lines are precipitation and vertically-integrated moisture for steady-state conditions,
1896 while the dashed blue and black lines correspond to precipitation and vertically-
1897 integrated moisture "smeared out" in the presence of time-varying, transient behavior.
1898 Adapted from Figure 2 of Lintner and Neelin (2009). (b) Rainfall longitudinal transects
1899 from the Climate Anomaly Monitoring System (CAMS) raingauge-derived precipitation
1900 data for September-October-November for the period 1950-2000 for El Niño (red), La
1901 Niña (blue), and all (black) years, averaged over 3.75°S-1.75°S. From Figure 4b of
1902 Lintner and Neelin (2007).

1903 Figure 14: Mesoscale heterogeneity impact on cloud generation in the dry season. a)
1904 Typical perspective regarding the impact of deforestation and clearings generating deep
1905 convective clouds and b) more realistic impact, in terms of mostly a modification of
1906 shallow convection cloud cover, impacting radiation more than precipitation.

1907 Figure 15: MODIS visible image of the Northwestern Amazon as the basin transition into
1908 the wet season. In the dry season surface heterogeneity whether due to rivers, forest-
1909 deforested patches or land-ocean contrast are very clear. In the wet season those sharp
1910 gradients disappear as cloud cover mostly dominated by deep convection starts
1911 organizing at scales independent from the surface heterogeneity.

1912 Figure 16: Continental recycling ratio, ρ, and recycling length scale, λ, normalized by
1913 length scale, L, along the inflow direction x for atmospheric moisture either increasing or
1914 decreasing along the inflow path in the idealized model of Schäfli et al. (2012). ρ
1915 represents how much of the rainfall is derived from terrestrial evapotranspiration, while λ
1916 represents the length scale over which evapotranspired water is removed from the
1917 atmosphere via precipitation. Generally ρ increases for larger distances into the
1918 continental interior, meaning recycling increases in importance, while λ decreases. From
1919 Figure 8 of Schäfli et al. (2012).

1920 Figure 17: 10 day-back trajectory analysis over several regions of the continental tropics,
1921 along with LAI, mean TRMM estimated rainfall, and GLDAS ET estimates.
1922

1923 Figures

1924
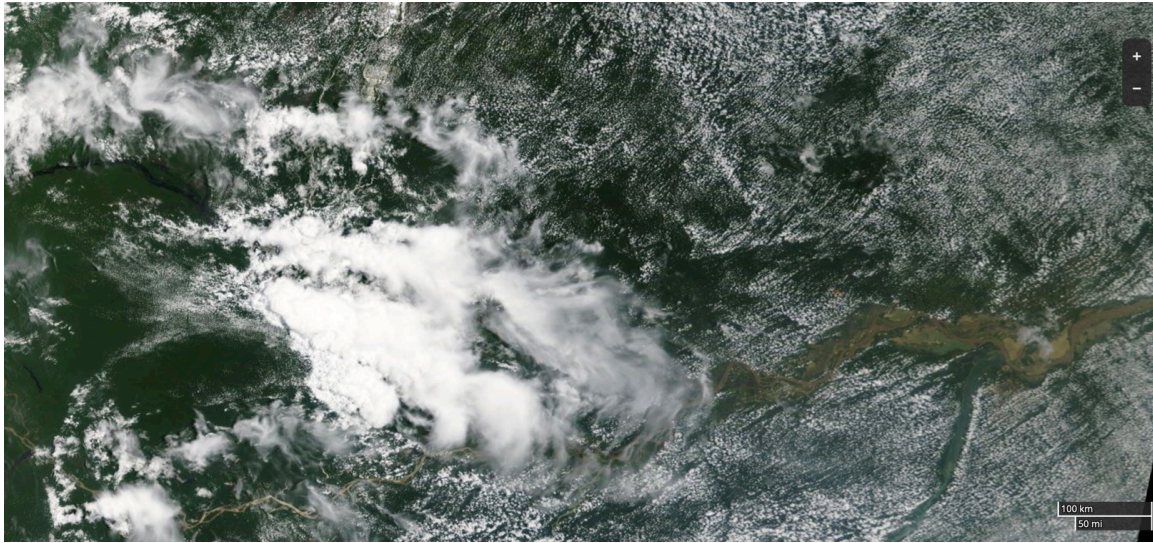
1925

1926 Figure 1: Snapshot of cloud cover over the Amazon basin on 2018, Sept 25 (courtesy
1927 NASA Earth Observatory, MODIS visible bands). Small clouds are shallow convective
1928 clouds, highlighting surface Bowen ratio changes between the river and the forest. On the
1929 left, the deep convective cells do not follow the surface heterogeneity (and is much larger
1930 in scale). Not the cold pool bow effect on the bottom left corner, with no clouds sithin the
1931 cold pools and clouds on the edge of the cold pool.
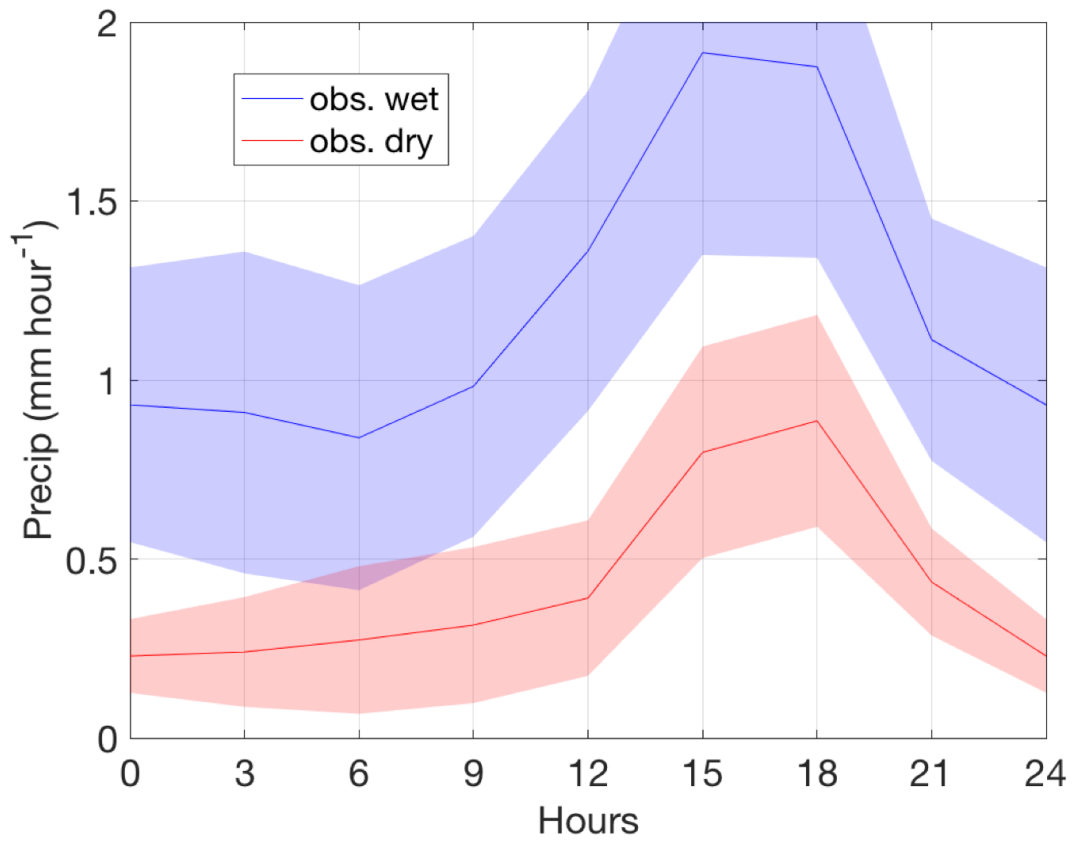
1932

1933 Figure 2: Diurnal cycle in local hour of dry (red) and wet (blue) season observations of

1934 precipitation at K34, near Manaus, along with their standard deviation averaged across

1935 years 2010-2014.

1936

1937
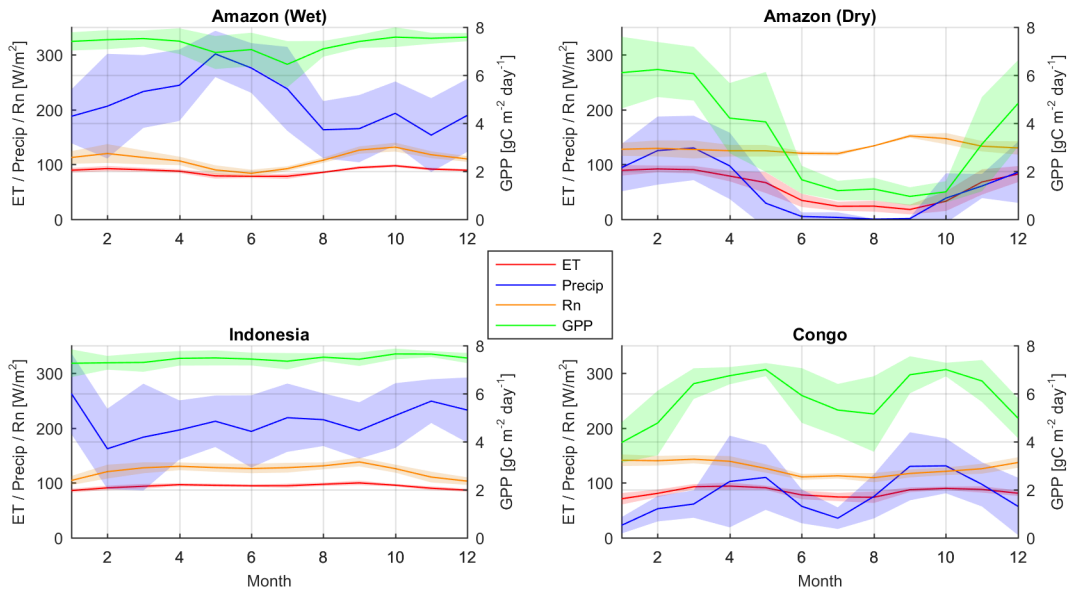
1938

Figure 3: Seasonal variations in Evapotranspiration (ET) from WECANN, Precipitation (Precip) based on GPCP in units of energy (W/m², by multiplying it by the latent heat of vaporization), Net Radiation (Rn) from CERES and Gross Primary Production (GPP) based on WECANN informed by Solar-Induced Fluorescence (SIF) over the wet part of the Amazon (top left), the Savanna region of Brazil (top right), over Indonesia (bottom left) and over the Congo basin (bottom right).

1945

1946
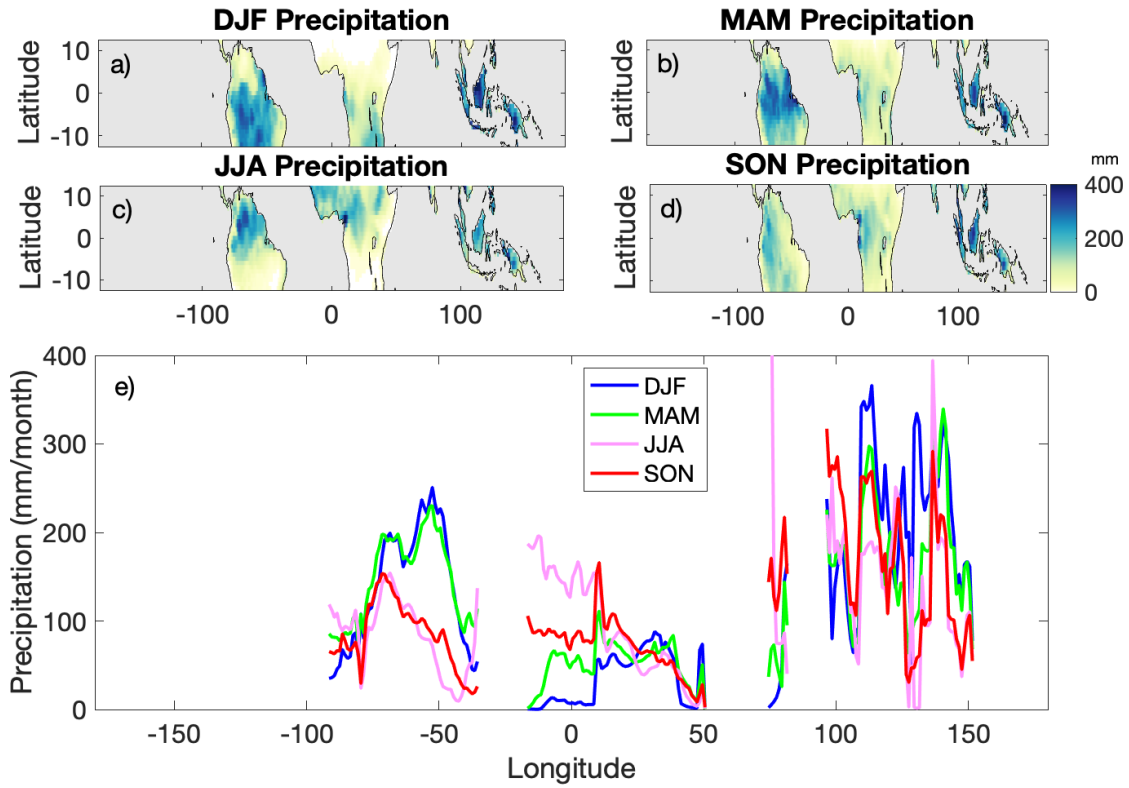
1947

Figure 4: Seasonality of Precipitation based on GPCP in the tropics in December-January-February (a), March-April-May (b), June-July-August (c), and September-October-November (SON) and its latitudinal average (e).

1951
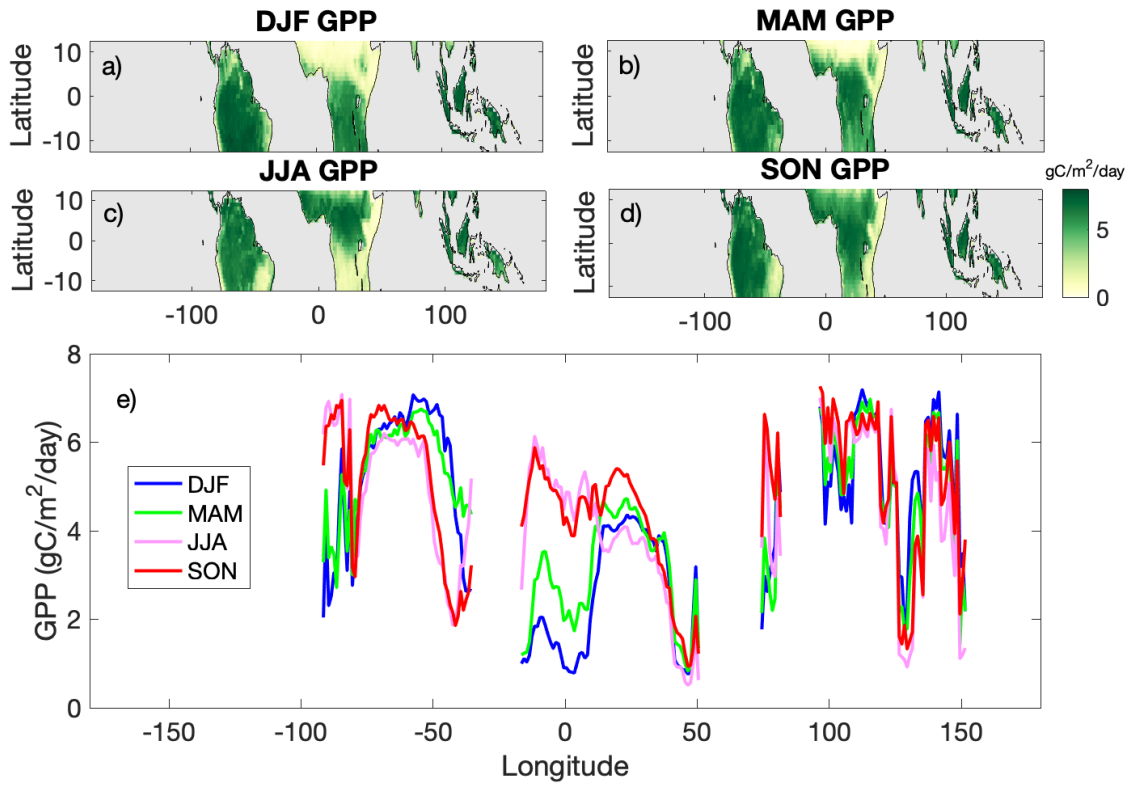
1952

1953   Figure 5: same as Figure 4 but for Gross Primary Production (GPP)

1954

1955
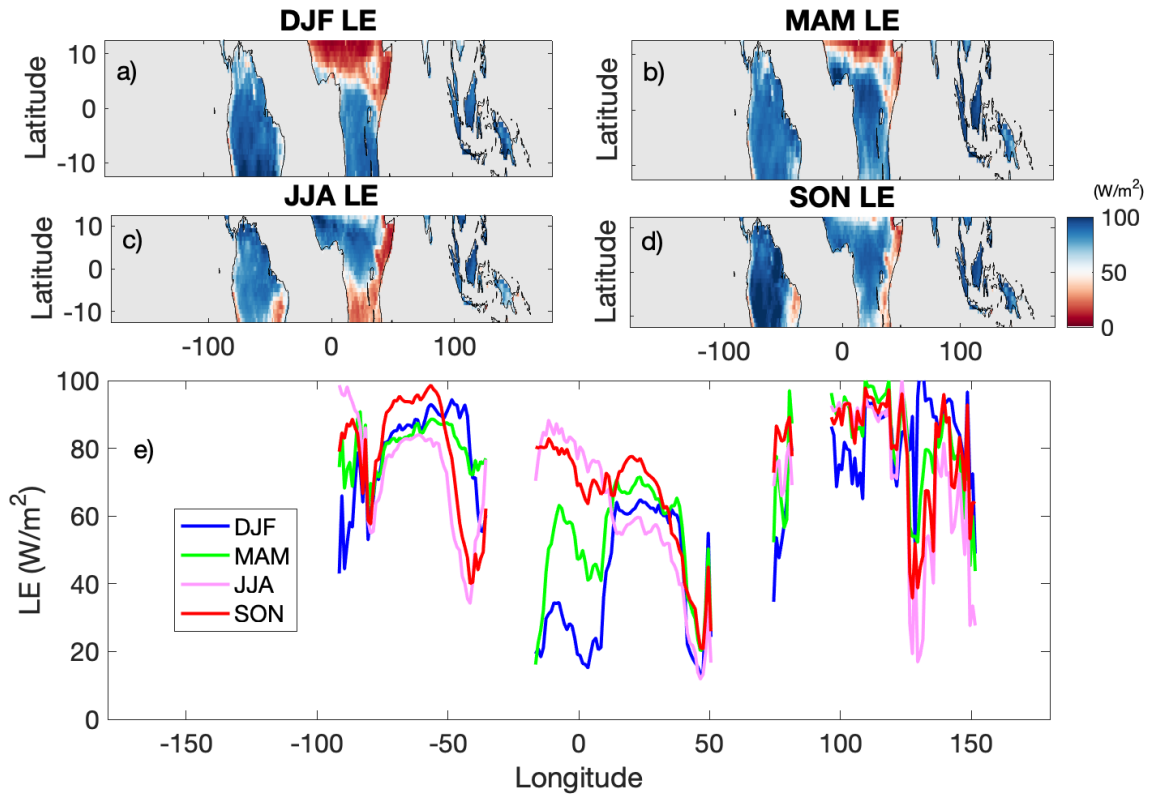
1956

1957   Figure 6: same as Figure 4 for latent heat flux LE

1958
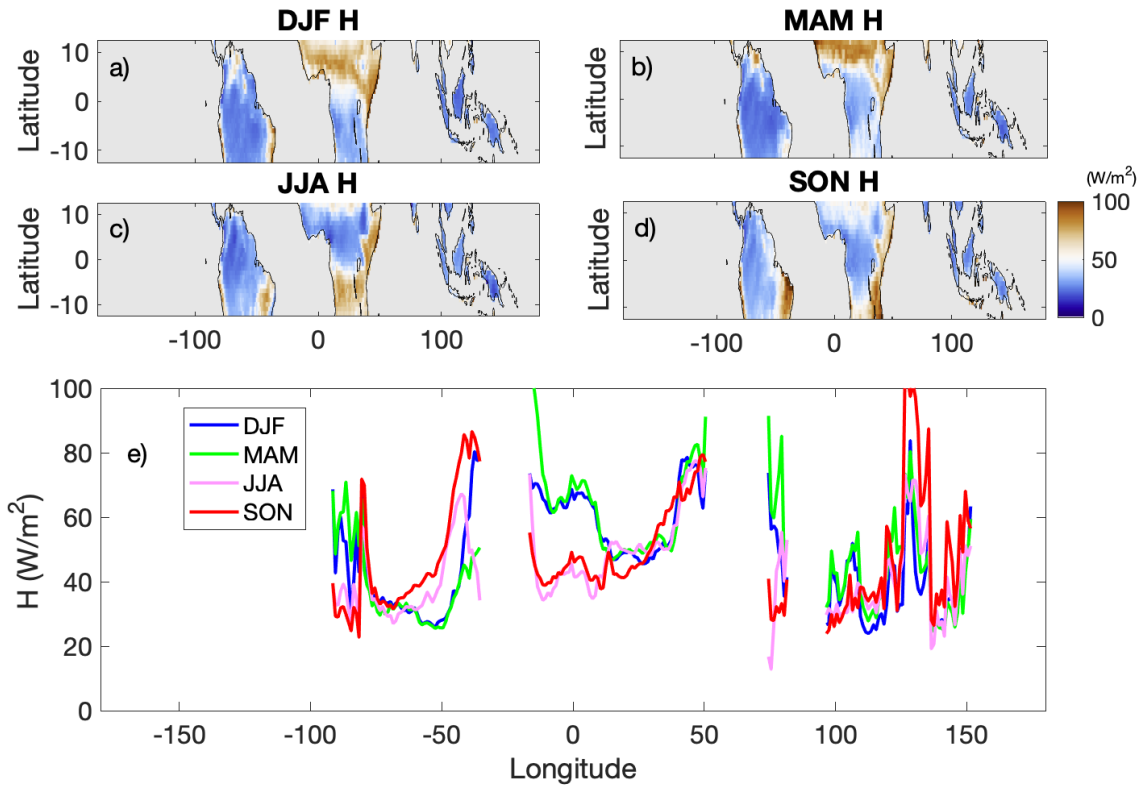
1959

1960   Figure 7: same as Figure 4 for sensible heat flux H

1961

1962
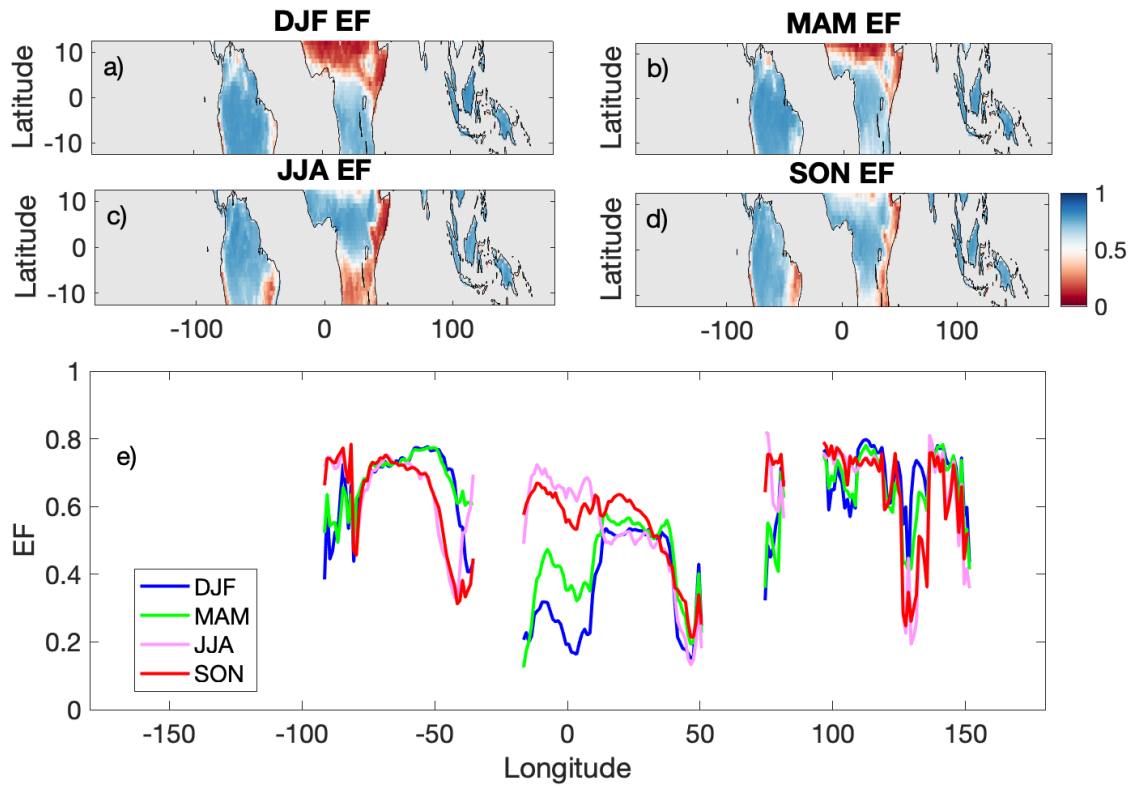
1963

1964 Figure 8: same as Figure 4 for evaporative fraction (EF), the ratio of LE to H+LE.

1965

1966

1967

1968
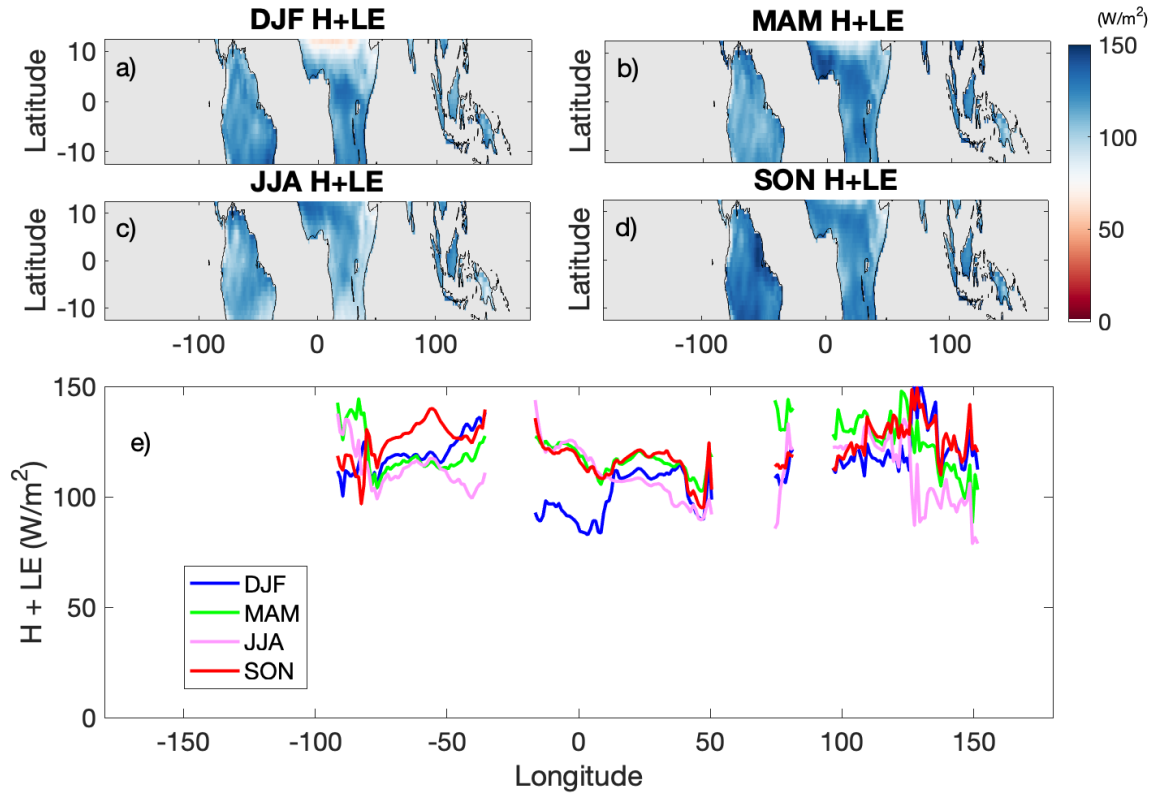
1969

Figure 9: same as Figure 4 for sea-level surface moist static energy flux, the sum of

sensible heat flux H and latent heat flux

1972

1973

1974

1975
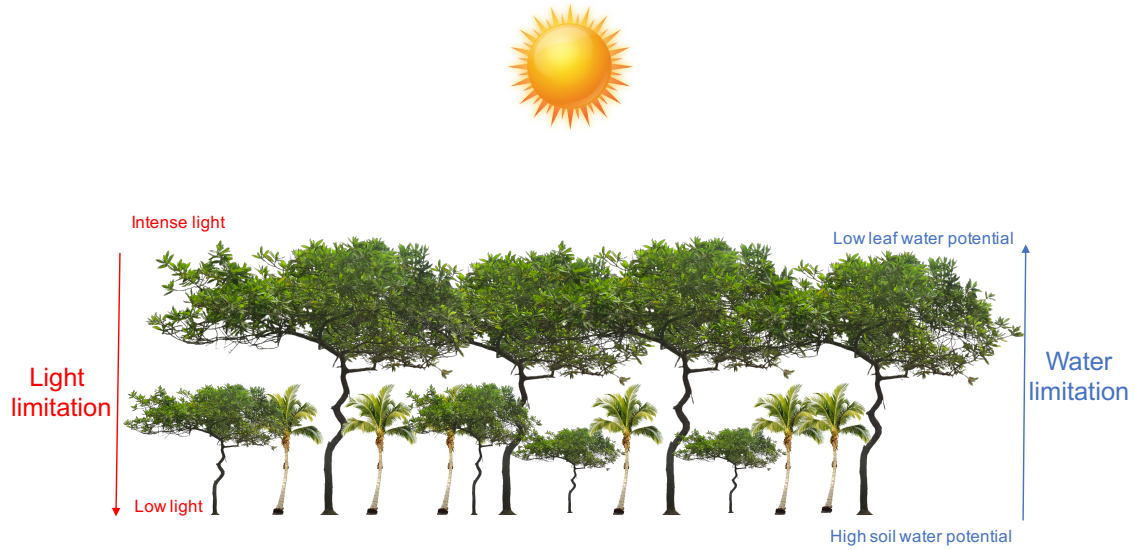
1976

1977 Figure 10: Schematic showing the vertical structure of light and water limitations in a
1978 tropical forest.

1979
1980
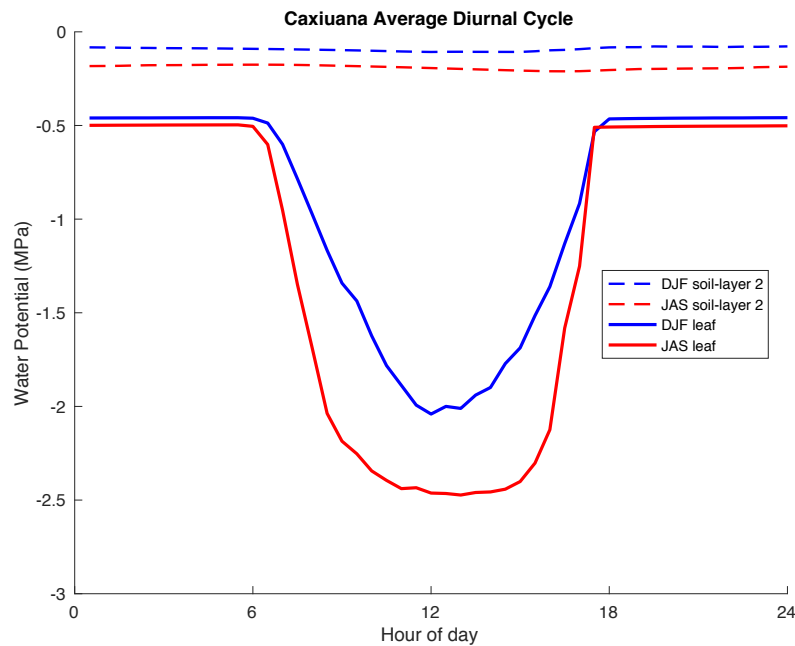
1981

1982 Figure 11: Climatology of the diurnal cycle of leaf water potential and top soil water
1983 potential in the dry and wet seasons in Caxiuana, Brazil simulated by the Community
1984 Land Model (CLM) with plant hydraulics.

1987
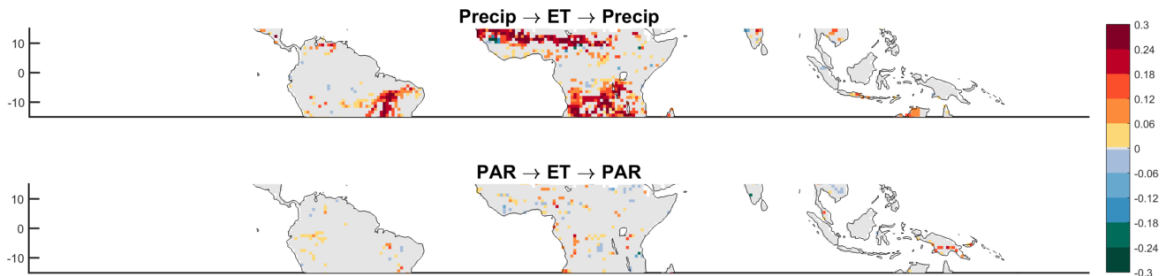
Figure 12: Land-atmosphere feedback strength (change in the variance due to the feedback) between Precipitation and ET (top) and Photosynthetically Active Radiation (PAR) (bottom) based on recent metric developed by Green et al. [2017] using a multivariate Granger causality approach.

1992
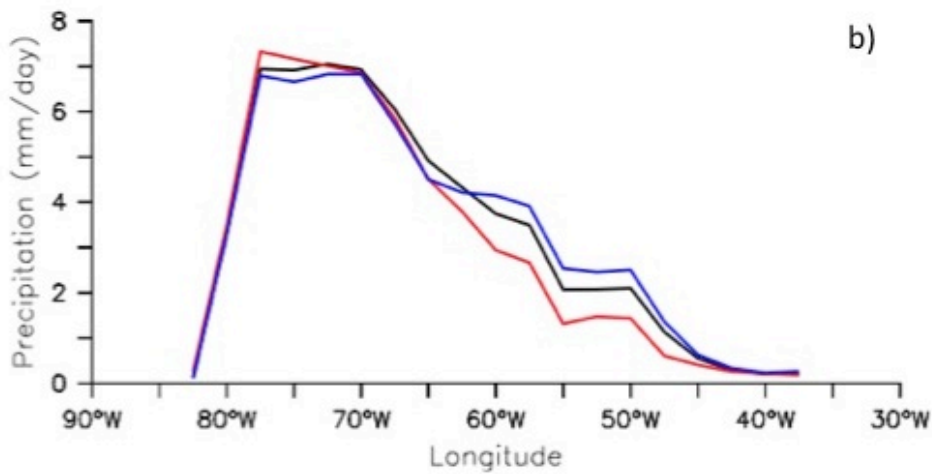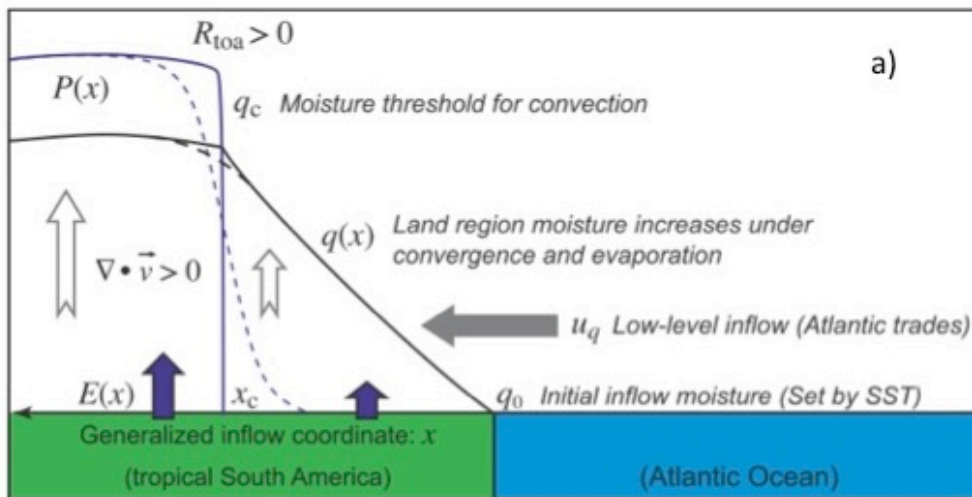
1993

1994   Figure 13: (a) Schematic of the key elements of the convective margins framework as
1995   applied along an inflow path across northeastern South America. The solid blue and
1996   black lines are precipitation and vertically-integrated moisture for steady-state conditions,
1997   while the dashed blue and black lines correspond to precipitation and vertically-
1998   integrated moisture "smeared out" in the presence of time-varying, transient behavior.
1999   Adapted from Figure 2 of Lintner and Neelin (2009). (b) Rainfall longitudinal transects
2000   from the Climate Anomaly Monitoring System (CAMS) raingauge-derived precipitation
2001   data for September-October-November for the period 1950-2000 for El Niño (red), La
2002   Niña (blue), and all (black) years, averaged over 3.75°S-1.75°S. From Figure 4b of
2003   Lintner and Neelin (2007).

2004

2005
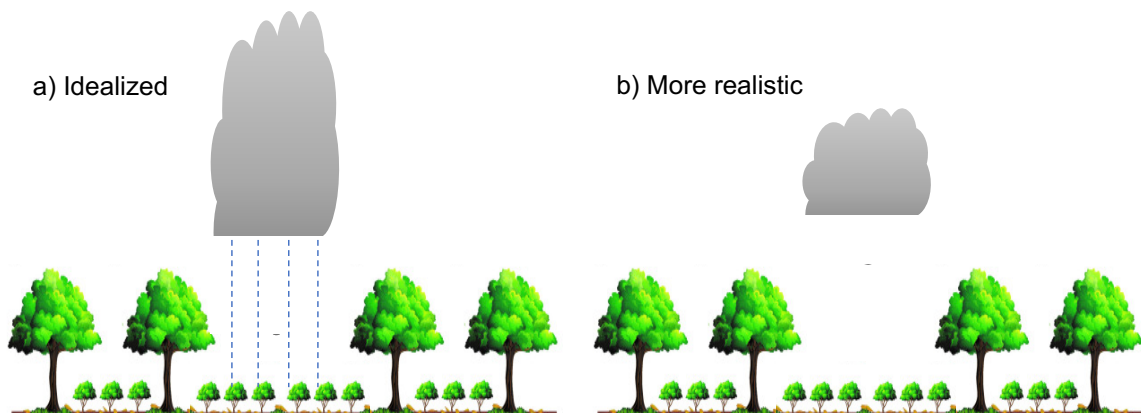
2006

2007   Figure 14: Mesoscale heterogeneity impact on cloud generation in the dry season. a)
2008   Typical perspective regarding the impact of deforestation and clearings generating deep
2009   convective clouds and b) more realistic impact, in terms of mostly a modification of
2010   shallow convection cloud cover, impacting radiation more than precipitation.

2011

2012

2013

Figure 15: MODIS visible image of the Northwestern Amazon as the basin transition into the wet season. In the dry season surface heterogeneity whether due to rivers, forest-deforested patches or land-ocean contrast are very clear. In the wet season those sharp gradients disappear as cloud cover mostly dominated by deep convection starts organizing at scales independent from the surface heterogeneity.

2014
2015
2016
2017
2018

2019

2020
2021
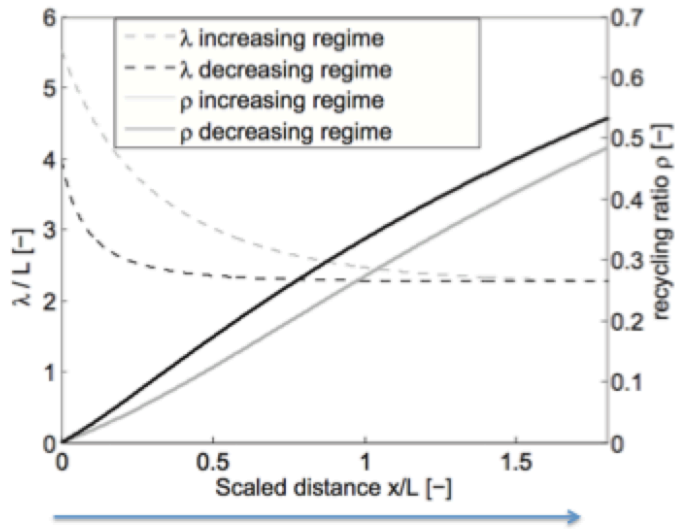
2022

2023 Figure 16: Continental recycling ratio, ρ, and recycling length scale, λ, normalized by

2024 length scale, L, along the inflow direction x for atmospheric moisture either increasing or

2025 decreasing along the inflow path in the idealized model of Schäfli et al. (2012). ρ

2026 represents how much of the rainfall is derived from terrestrial evapotranspiration, while λ

2027 represents the length scale over which evapotranspired water is removed from the

2028 atmosphere via precipitation. Generally ρ increases for larger distances into the

2029 continental interior, meaning recycling increases in importance, while λ decreases. From

2030 Figure 8 of Schäfli et al. (2012).

2031
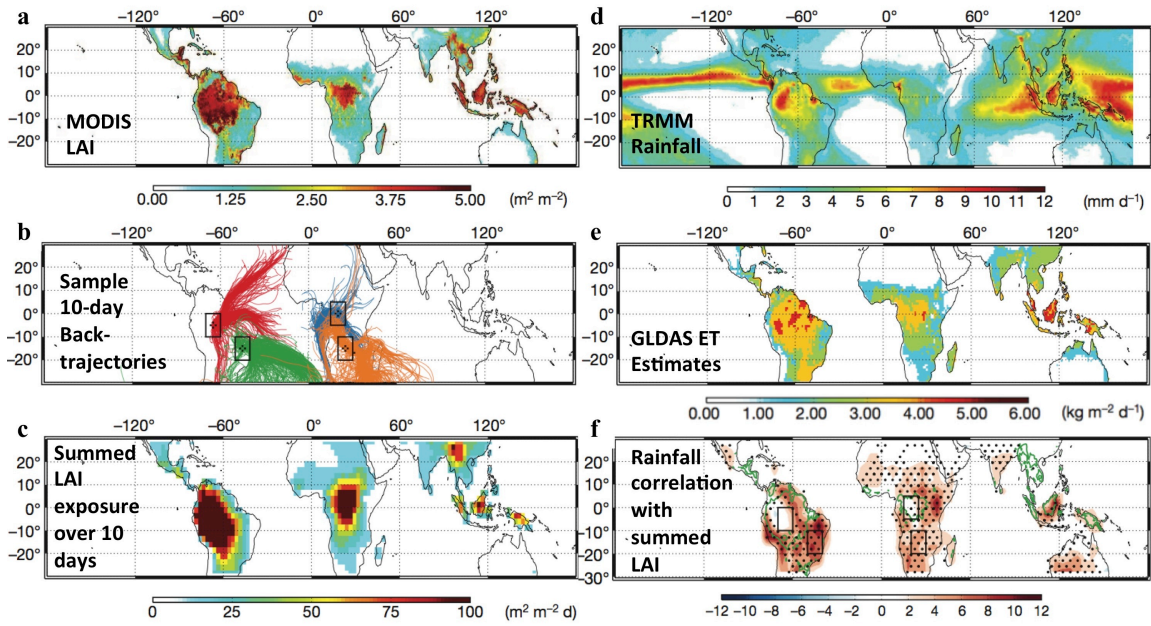
2032

Figure 17: 10 day-back trajectory analysis over several regions of the continental tropics, along with LAI, mean TRMM estimated rainfall, and GLDAS ET estimates.

2033

2034

2035

2036

2037

2038

2039

2040